Operating a Zero Carbon GB Power System in 2025: Frequency and Fault Current

Power Electronic Devices and Fault Current

Contributors

Shuren Wang

Agusti Egea-Alvarez

Date: 4th April 2020

Contents

1 Introduction and Executive Summary

Power electronics play a key role in the integration of renewable energy into the power system, as the major part of renewable energy devices have different voltage and frequency requirements and cannot be directly connected. The power converter acts as an interface optimising the power extracted from the renewable energy source (RES) and, at the same time, it provides grid support and ensures compliance with grid code. Power electronic converters, compared to synchronous machines, present different dynamic characteristics, one of which is that they cannot be overloaded. If more current is needed, the power converter must be oversized; this will have a definite impact on the cost. This report explains power converter limitations and behaviour during faults. This report also provides an economic assessment of the different converter technologies to inform estimates of the likely cost of using oversized power converters to provide fault current.

This report describes the following:

- The most common power electronic converters for grid-connected applications
- Power semiconductors characteristics and safe operation area (SOA)
- Main aspects of converter design and optimisation
- Grid-connected converter control strategies and the impact of the fault ride through strategy during faults
- Converter fault ride-through during the ac grid fault
- Cost assessment of grid-connected power converters.

This report discusses the fault current provision of the grid-tied power electronic converters, regarding system configuration, fault ride-through behaviour, converter limitations, control systems and cost aspects. The main findings can be summarised as:

- There are different power converter solutions (topologies) for the grid-tied applications, depending on the energy sources and/or grid requirements. Two-level power converters are used in low power and voltage applications and multilevel converters are used in high voltage and mid to high power applications.
- Power semiconductor has to operate within its safe operating area (SOA), where the voltage, current and power capabilities are defined. If the converters' current, voltage or power exceeds the SOA, the power semiconductor can be destroyed.
- The converter's SOA is further limited by the systematic safe operating area (SSOA). As large current and voltage transients exist in the converter, the power semiconductor SOA is further limited to allow room for the current and voltage transients.
- A proper electromagnetic and thermal design could be helpful for the maximum utilisation of the semiconductor power capability. However, there is limited potential for converter optimisation which aims at enlarging the semiconductor capability, due to the fast nature of the transients.
- With the implementation of current control, the power converters have the capability to control its AC side current and limit the current in case of fault. Allowing the converter to continue operating in case of fault. Converter control could help in the development of solutions to approach the grid code requirements.
- RES developers could choose to oversize their power converters in order to provide fault current. The additional cost is likely to be proportional to the added kW capacity. Based on the literature, power converters and other related components for grid-tied applications have a cost around £0.04-0.1k/kW, (equivalent to 3% of the turbine cost for onshore or 5% for offshore) which are proportional with the

power ratings; therefore, increasing the current capability of the power converter generally implies increasing the cost linearly.

- Further work on determining the feasibility of oversizing converters to provide overcurrent during faults should be done alongside wind plant original equipment manufacturers (OEMs).

2 Introduction to Power Converters for Grid-Connected Applications

2.1 Power Converter Topologies

Different power converter topologies are used in grid-connected applications. For low voltage and low power applications, the most commonly used topology is the two-level converter. This can be found in the major part of existing wind turbines and solar systems. When the power level increases, other power converter topologies might be used to reduce the power loses. Multi-level converters, such as a three-level converter, are starting to be used in large wind turbines and medium voltage applications. For HVDC links, the preferred technology is the modular Multi-level converter (MMC) that can be seen as the connection in series of small two-level converters (up to 500 submodules). Modular Multi-level converter technology represents a more efficient and controllable technology compared to two-level converters. A classification of the different power converters can be seen in Table 2.1.

Table 2.1: Classification of the grid-connected VSCs [1]–[3].

Waveform Characteristics and Level	**Converter Types**	**Phase Number**
Two-Level Converter [1]	Standard two-level converter	Single and three-phase
Multi-Level Converter [2], [3]	Neutral-Point Clamped Converter (NPC) Flying-Capacitor Converter (FCC)	Three-phase
Modular Multi-level Converter [2], [3]	Half-bridge MMC, Full bridge MMC	Three-phase

2.1.1 Two-Level Converter

A three-phase two-level VSC is illustrated in Figure 2.1. This is the most common power topology used in electrical drives as well as low power (below 10 MW) generation applications. A two-level power converter is composed of six power electronics switches, two for each phase and connecting the DC link with the phase. A power converter has the function to inject the desired active and reactive current. This is achieved opening and closing the switches above 1 kHz. The binary signal to command the switches is calculated as the comparison of the desired voltage waveform and a carrier signal. This technique is called PWM [4].

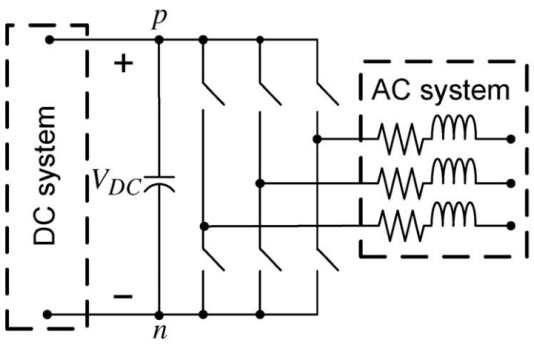

Figure 2.1: A three-phase two-level VSC connecting to a three-phase ac system [3].

Figure 2.2 presents an example of the PWM for one phase when the carrying signal is below the voltage reference, the power electronics switches are fired. In this way, a sinusoidal waveform can be synthesised using a power electronics

device that only has ON/OFF state. The PWM process generates harmonics and extra filtering equipment might be required at the power converter terminals. At higher switching frequencies, the harmonic pollution is reduced but, at the same time, the switching actions implies some power losses that increases when the switching frequency increases.

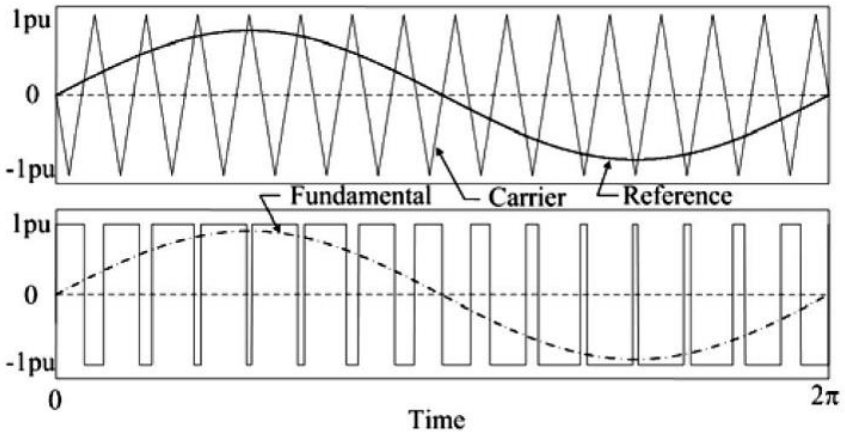

Figure 2.2: PWM and voltage generation illustration one phase of two-level VSCs [4].

2.1.2 Multi-Level Converters

Multi-level converters are devices that can synthesise more than two voltage levels, which is especially attractive in high-voltage/power applications [2] reducing the loses as well as the harmonic emission. Three multi-level converter topologies are given in Figure 2.3.

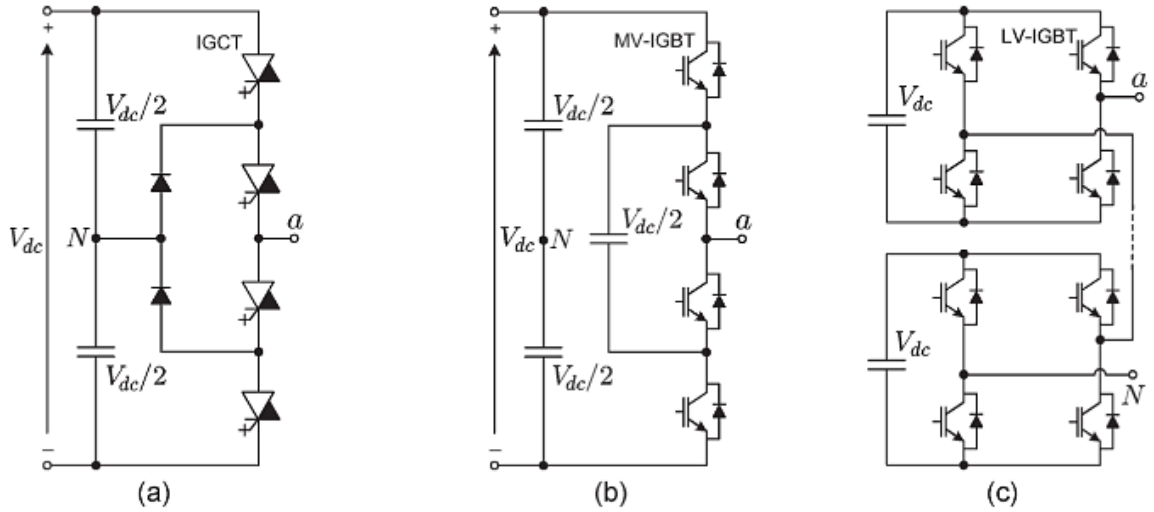

Figure 2.3: Classic Multi-level converter topologies (with only one phase shown). (a) Three-level NPC with IGCTs. (b) Three-level flying capacitor converter with IGBTs. (c) Five-level cascaded H-bridge [5].

Figure 2.4 shows the output waveforms of three-level and five-level converters. Therefore, high voltage ratings can be reached with the same semiconductor devices.

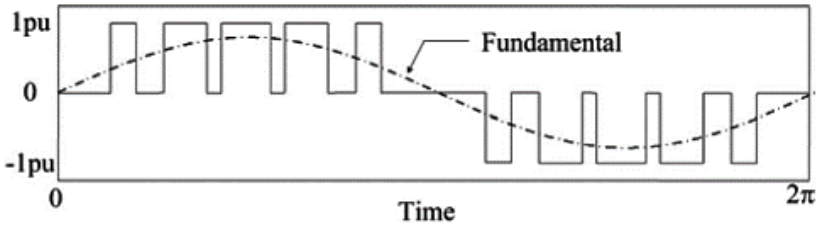

(a) Three-level output waveform

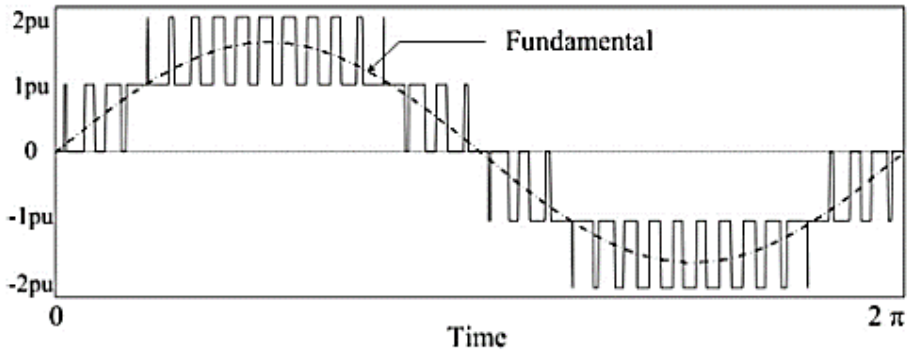

(b) Five-level output waveform

Figure 2.4: Multi-level output voltage waveforms [4].

MMC is another Multi-level converter type, which is shown in Figure 2.5. It can be seen that MMC consists of submodules (SMs) with two switches and a capacitor each and two arm reactors per phase [6]. Theoretically, MMC can achieve high-voltage application without limitation; therefore, it is suitable for high-voltage and high-power scenarios. However, it involves a large number of semiconductor devices, thus cost aspect should be considered in particular. This topology is used mainly for HVDC systems.

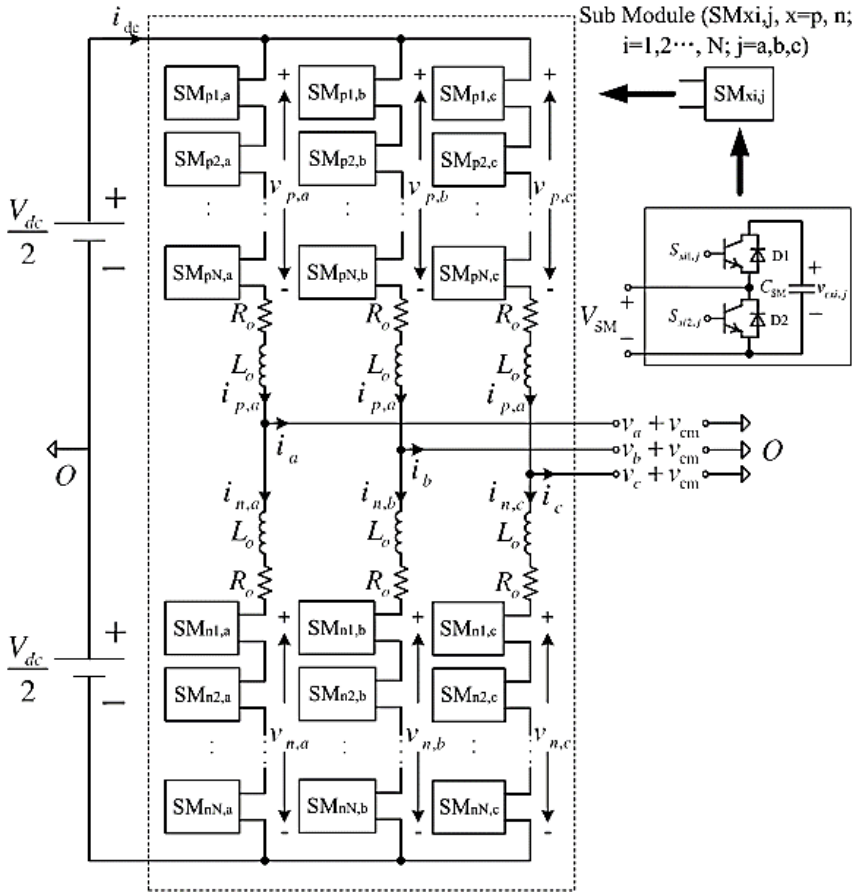

Figure 2.5: An MMC topology with high-bridge SMs [7].

2.1.3 Converter Classification

Table 2.2 lists the main area and applications that grid-connected power converters are used highlighting the most common used topologies.

Table 2.2: Studied grid-tied applications.

Area	Applications	Converters	
Renewable Power Generation	Wind Power	Three-Phase	Two-Level Converter (<10MW) Multi-Level Converter (>10MW)
	Solar Power	Single and Three-Phase	Two-Level Converter
	Distributed Generation	Single and Three-Phase	Two-Level Converter
Grid Application	STATCOM	Three-Phase	Two-Level, Multi-Level Converter, MMC
	HVDC	Three-Phase	MMC

2.2 Power Converter Grid-Tied Applications

This subsection summarises the most common grid-connected power converter applications, including wind and solar power generation, HVDC and STATCOMs.

2.2.1 Wind Power Generation

Modern wind turbines are complex mechanical and electrical systems where power converters are required to interface the wind turbine generators (WTGs) and the power network maximising the power extraction as well as be grid compliant. Turbines are classified into fixed speed (Type 1), limited variable speed (Type 2), or variable speed with either partial (Type 3) or full (Type 4) power electronic conversion [8]. Among these types, types 3 and 4 are the most common type of wind turbines and are equipped with power electronic converter to maximise the power generation and support the electrical system, as shown in Figure 2.6.

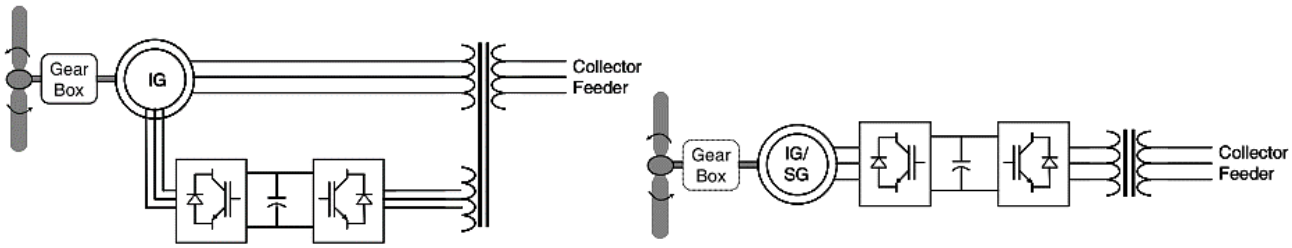

(a) Type 3 (b) Type 4

Figure 2.6: Typical configurations of WTG [8].

Type 3 turbine, known commonly as the doubly-fed induction generator (DFIG) is based on a wound rotor induction machine. The rotor windings are supplied via slip rings by a voltage-source converter, which can adjust the rotor currents' magnitude and phase nearly instantaneously. This rotor-side converter is connected back-to-back with a grid side converter, which exchanges power directly with the grid. The Type 4 turbine is an evolution of Type 3 and a full-power converter is used to interface the electrical generator (either induction generator or synchronous generator). All the power is processed through a full-scale back-to-back power converter. In Type 4 wind turbines gear-box may be eliminated, as there is no need for the generator to rotate at grid frequency. This supposes an advantage as the wind turbine powertrain can be simplified.

In terms of reactive power capability, Type 3 WTGs typically have a standard reactive power capability corresponding to a power factor of 0.95 lagging (capacitive) to 0.90 leading (inductive) [9]. For Type 4, the reactive power support can be extended and grid side converter can be used as STATCOM when no active power is generated.

2.2.2 Solar Power Generation

In order to integrate solar power into the electric grid, various power converter configurations are used, as shown in Figure 2.7 [10]. In a similar way as the wind farm, the power converter allows the optimal extraction of power as well as be compliant with the grid codes. The photovoltaic (PV) panels can be connected to the grid with a centralised inverter, as shown in Figure 2.7(a); if this inverter presents a malfunction, the whole PV system will be disconnected from the grid. Modularized systems are shown in Figure 2.7(b) and Figure 2.7(c) tend to increase the reliability of the system since a faulty converter or PV module can be disconnected from the system while others can operate continuously [10] but this systems are more expensive and present more losses.

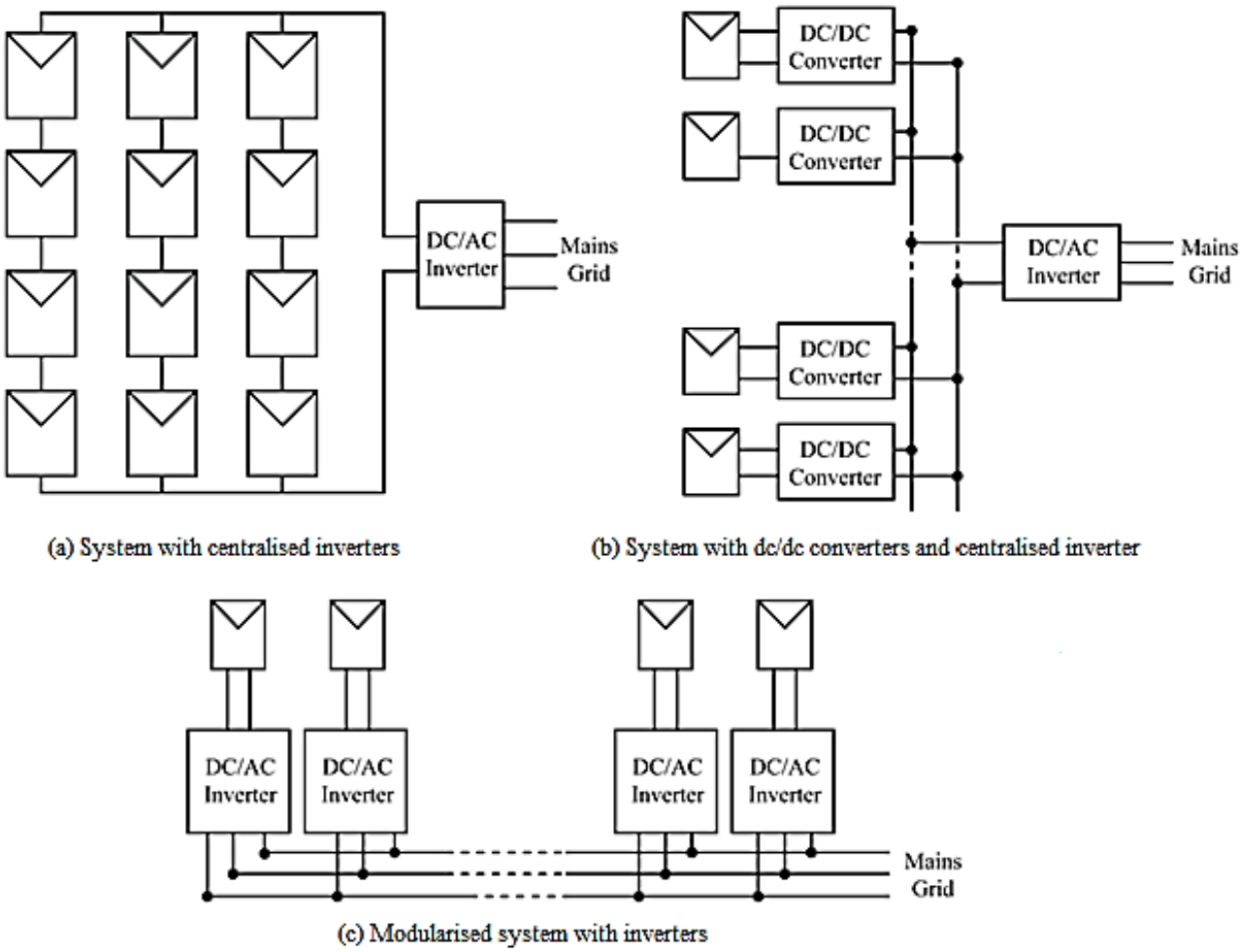

Figure 2.7: Grid integration of PV systems [10].

2.2.3 High Voltage DC System (HVDC) Technology

HVDC systems are used to transfer large amounts of power when AC transmission systems are not efficient such as power transfer covering long distances or offshore connections. HVDC can be implemented using current source converters (thyristors) or voltage source converters (transistors) [11]. A typical HVDC transmission scheme is shown in Figure 2.8, where two grids are connected via power converter stations and transmission lines/cables.

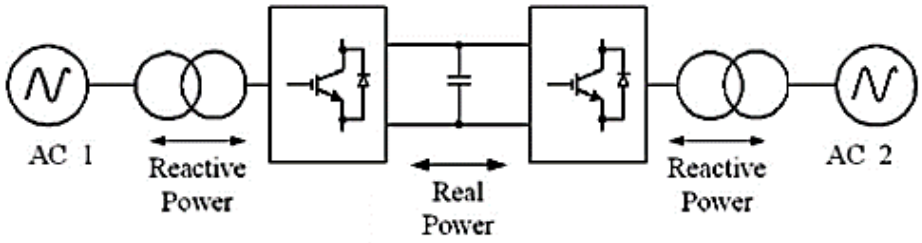

Figure 2.8: A point-to-point VSC-HVDC transmission configuration [4].

Besides point-to-point power transmission, VSC-based system enables interconnection of a number of terminal stations, as shown in Figure 2.9. In this way, the robustness and reliability of the overall system increase.

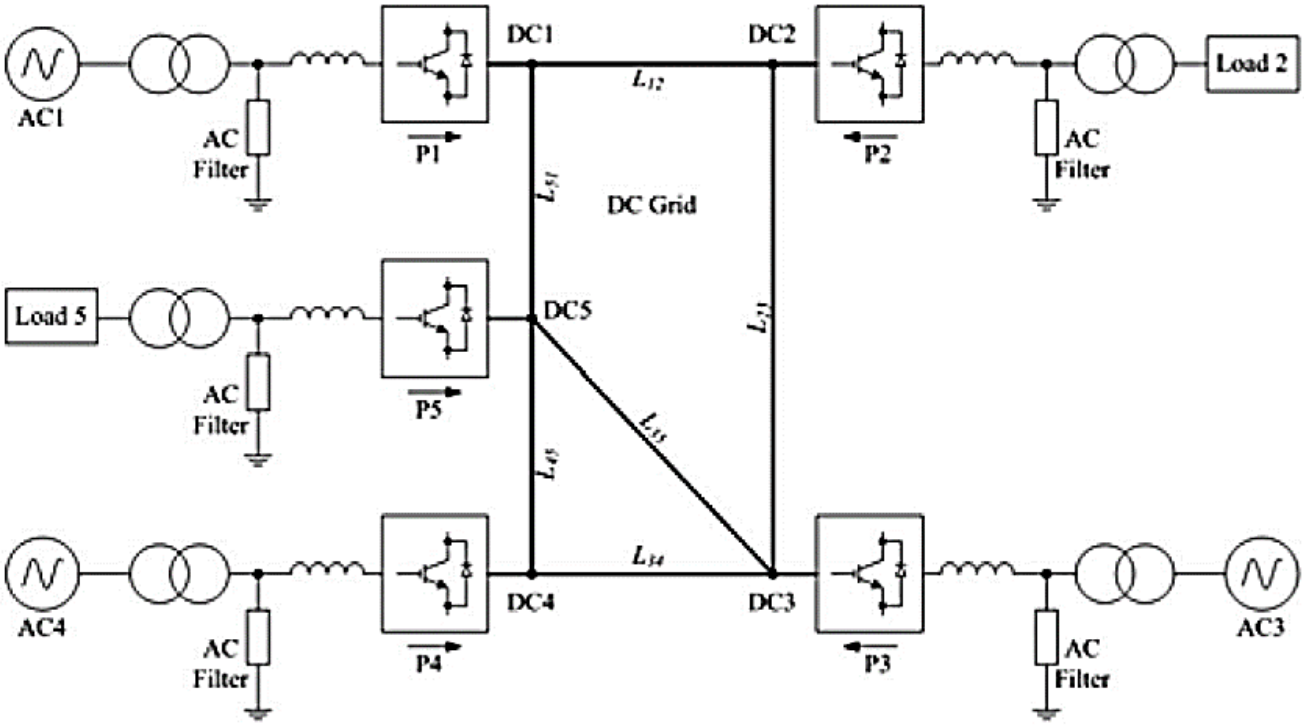

Figure 2.9: A five-terminal VSC-HVDC transmission system [4].

Different grid-connected power converter topologies could be used in HVDC systems, varying from two-level converters to Multi-level converters. Notably, the MMC is a promising topology in this field. Multiple functionalities, such as active/reactive power support, fault-tolerant operation and/or other ancillary services are required for the VSCs by the tied grids.

2.2.4 Static Compensator (STATCOM)

STATCOM is typically a VSC based system whose prime function is to exchange reactive power with the ac system, as shown in Figure 2.10. Two-level converter [12], neutral point clamped multi-level converter [13], and MMC are feasible choices as the power converter.

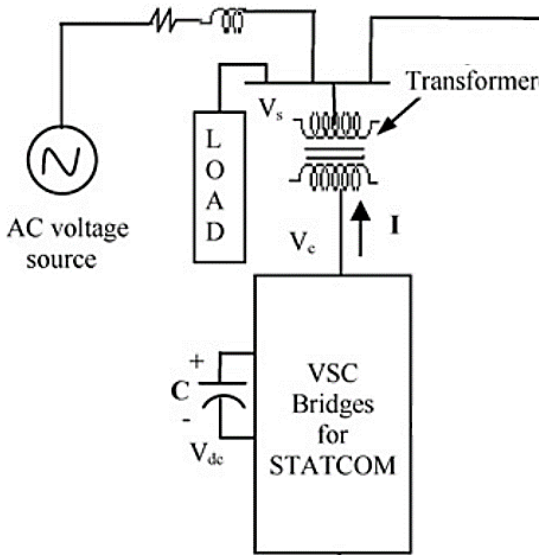

Figure 2.10: A VSC-based STATCOM configuration [14].

In an electric power transmission system, the STATCOM can be used to increase the line power transmission capacity, to enhance the voltage/angle stability, or damping the system oscillatory modes. In a distribution system, the STATCOM is mainly used for voltage regulation; however, it can also supply real power to the loads in the case of a blackout if it is augmented with an energy storage device, for example, a battery storage system [15].

3 Power Semiconductors

This section presents the basics of power semiconductors, and discusses the safe operation characteristics of the semiconductor devices of power electronics that would define the converter current and voltage limitations. Power switches are based on semiconductor materials and allow to control the ON/OFF state of the switch applying a current or voltage at the converter gate [1].

3.1 Introduction to Transistors

The two main transistors used in grid-connected power converter are: the metal oxide semiconductor field-effect transistor (MOSFET) and insulated gate bipolar transistor (IGBT). A MOSFET (n-channel) is shown in Figure 3.1, where terminals drain or input (D), gate (G) and source or output (S) are displayed. MOSFETs are usually commercially available with a diode in antiparallel for grid-connected applications. MOSFET is the fastest power switching device, with switching frequency up to MHz with voltage power ratings up to one thousand volts and current rating as high as one thousand amps [16] but the switching frequency is kept around 20 kHz for grid applications.

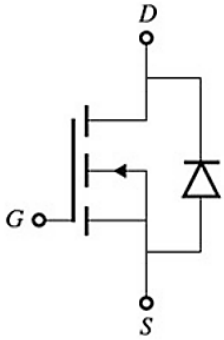

Figure 3.1: A MOSFET schematic.

The i-v characteristics MOSFET is shown in Figure 3.2, where the MOSFET can be controlled operating within linear, saturation and cut-off regions. For power applications, the MOSFET usually works in the cut-off region (near the X-axis, voltage V_{DS} is maximum) when is in off-state and in the linear region (near Y-axis, voltage V_{DS} is minimum) when is in on-state. The saturation region is usually used in small-signal but not in power applications.

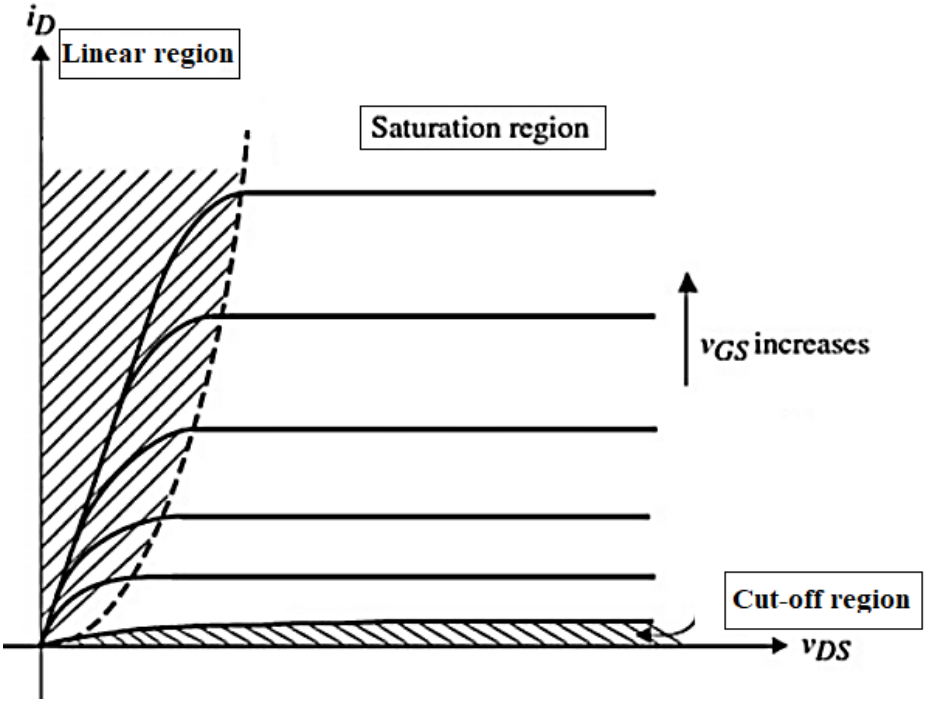

Figure 3.2: MOSFET i-v characteristics [16].

The other power switch that is commonly used for grid-connected applications is the insulated gate bipolar transistor (IGBT). Figure 3.3 shows the switch schematic where terminals collector or input (C), emitter or output (E) and gate (g) are displayed. Its i-v characteristic is similar to the MOSFET device in Figure 3.2. Usually, a diode is usually integrated into the practical IGBT packages, similar to that shown in Figure 3.1. IGBT can operate at frequencies lower than MOSFET and is available at ratings as high as several kVs and thousands of amps. This is the most common switch for grid-connected applications.

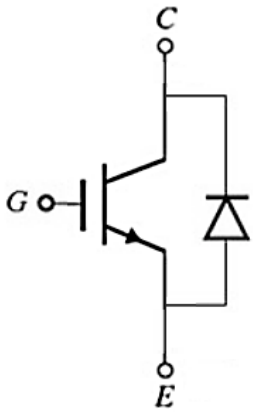

Figure 3.3: An IGBT schematic [16].

Figure 3.4 shows the electrical operating bounds of common semiconductor power switches, where the general trend is the higher the i-v ratings the slower the possible switching frequency, (because of increased losses associated with attaining higher sustaining voltages), hence increased junction temperature. High-frequency and low-power switching applications are dominated by the MOSFET while high-power low-frequency switching applications are dominated by thyristor type devices or more recently advanced IGBT modules. It should be noted that the voltage is restricted by silicon limitations while current is bounded by packaging and die size constraints [1].

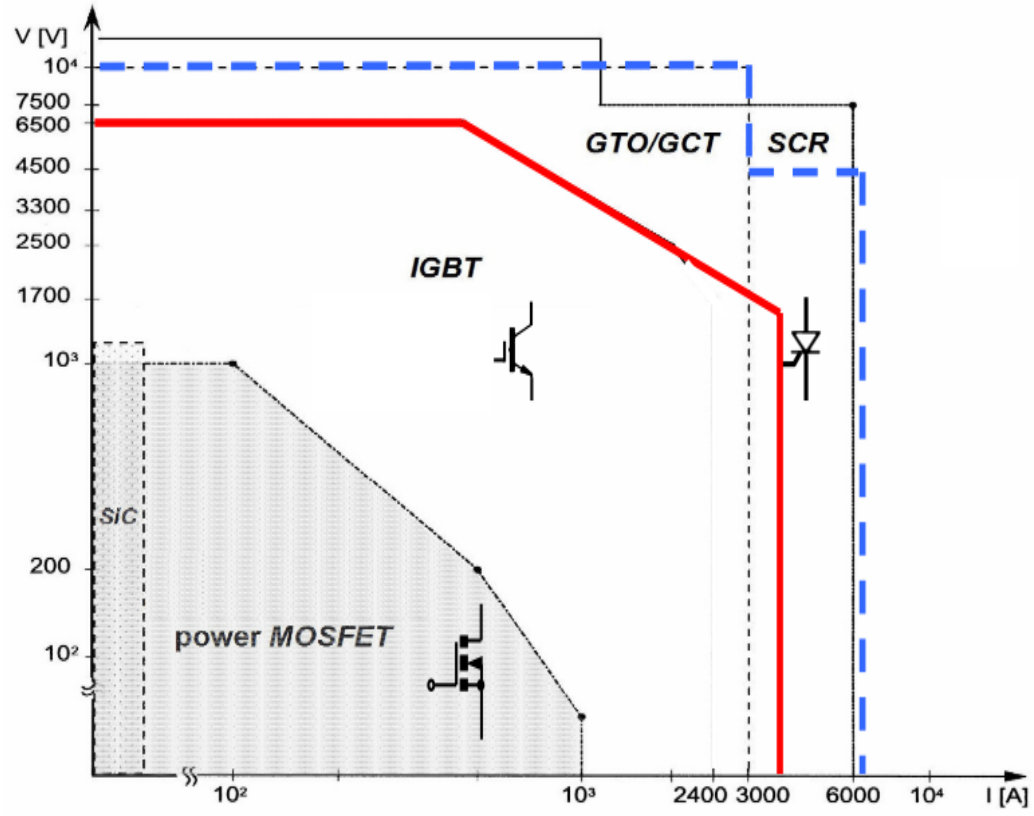

Figure 3.4: Electrical rating bounds for power switching silicon devices [1].

3.2 Safe Operating Area (SOA)

For a specific semiconductor device, the datasheet usually specifies the region in which the transistor can operate within its limits; the region is known as the safe operating area (SOA) [16]. It represents the permissible range of current, voltage, and power of the device when in operation and indicates that the current and voltage limits the device must handle to avoid destructive failure. SOA has no time dependency as an instantaneous overcurrent or voltage can destroy the semiconductor switch.

A generic SOA for a power semiconductor device is shown in Figure 3.5, where SOA bound is confined by four outer bounds labelled as A, B, C, and D, respectively:

- **Voltage limit (bound A)**: The bound A is specifying the break-down voltage rating, such as V_{DS} for MOSFETs and V_{CE} for IGBTs [1]. This bound defines the maximum voltage for a specific device.

- **Power limit (bound B)**: The bound B shows the area limited by the thermal dissipation, indicating the power handling capability. [17];

- **Current limit (bound C)**: The bound C is limited by the current rating of the device. For a given device, the maximum drain current (MOSFETs) and collection current (IGBTs) are usually defined by this line [18]. For a specific application with determined voltage rating, such a current bound shows the maximum current handling capability of the power converter;

- **Current limit (bound D)**: When the MOSFET is on, with minimum drain voltage at maximum drain current, it operates in the resistive mode where the drain current is given by $I_D = V_D/Ron$ [1]. Thus, the SOA region at high currents and low voltages is thus characterised by a line as the bound D. This area, which is reported by certain IGBT manufacturer, is also limited by the conduction loss V_{CE} at a maximum junction temperature of IGBTs [19].

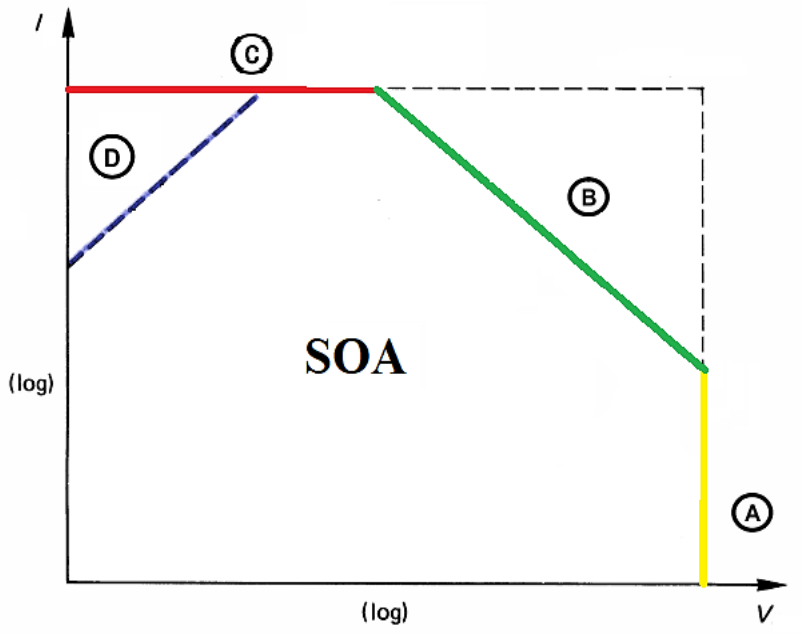

Figure 3.5: The SOA of the power semiconductor [1].

Depending on many factors, SOA may vary with semiconductor design and it is usually provided by the manufacturer [18]. Figure 3.6 shows an example of the trace that a switch does when switching on and off. As can be seen the switching has to be always within the area of the SOA.

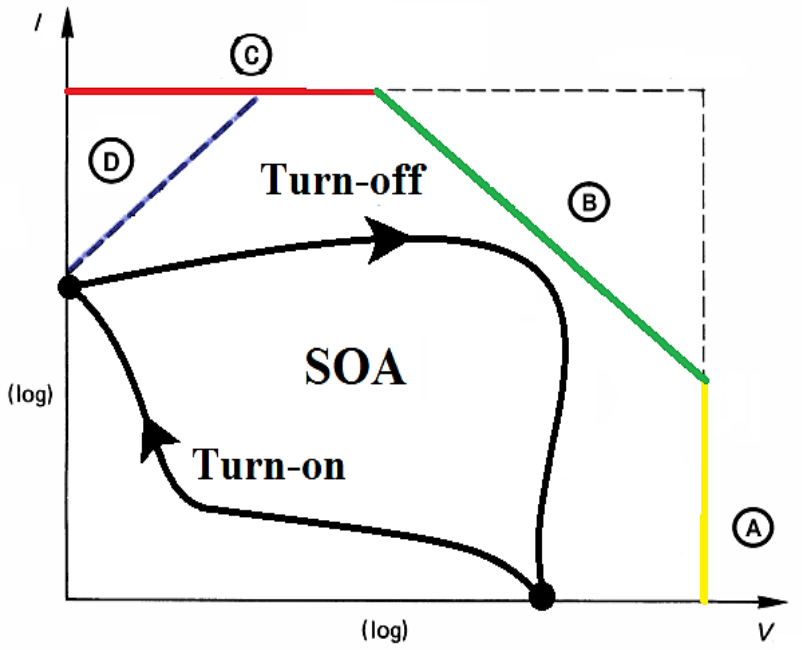

Figure 3.6: The power semiconductor operating trajectories within the SOA [18].

4 Limitations of the Semiconductor-Based Power Converters

Generally, the SOA reflects intrinsic characteristics of semiconductor devices but the area of operation must be further reduced when a power converter is designed. Large current and voltage derivative due to the switching action in combination with the parasitic inductances and capacitors produces large current and voltage peaks during the transients that should be taken into account during the converter design phase.

A study presented in [20] extends the device SOA concept to the power converter level, where the systematic safe operating area (SSOA) is for the power converter design, as in Figure 4.1. As can be seen, SSOA limits further the current and voltage operating area that a converter can operate in steady-state.

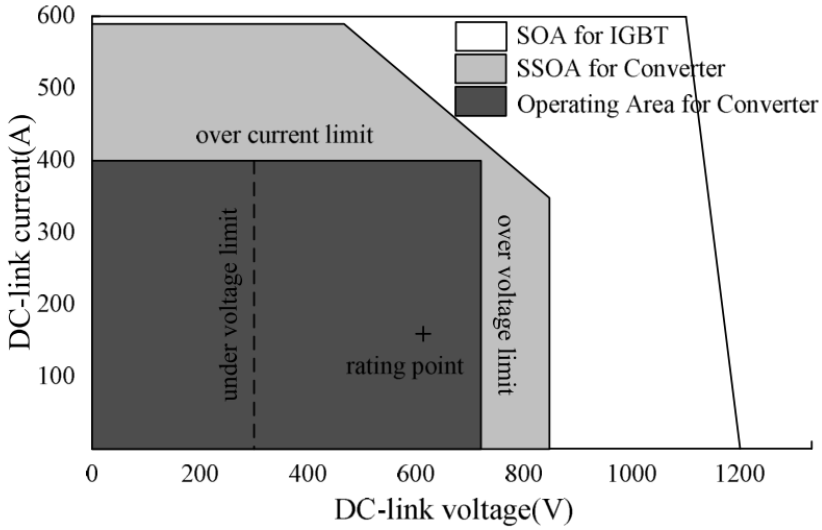

Figure 4.1: An SOA and SSOA example for power converter design [20].

4.1 Electromagnetic Limitations

In Power Electronics, the transient electromagnetic behaviours of the used power semiconductors pose many design challenges. This section clarifies why the SOA and SSOA of a power converter should be preserved and describes some of the design techniques.

4.1.1 Current and Voltage Limitations

Power semiconductors are commanded to open and close through gate pulses that can be seen as instantaneous steps. Such pulse transients impose high electric stresses, for example large di/dt, which could be coupled with the circuit parasitic inductance generating high voltage spike in the switching process. Figure 4.2 shows a turn-off procedure of a power semiconductor, where the parasitic inductance in the commutation loop causes a high voltage spike during the turn-off period.

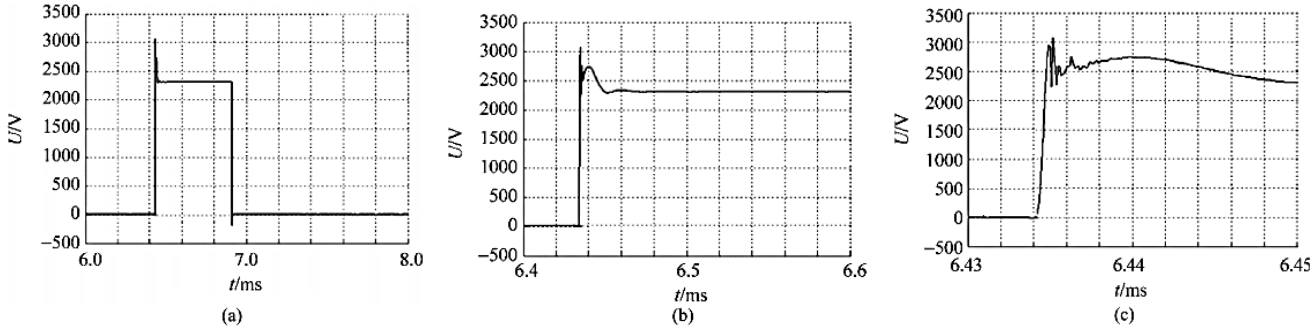

Figure 4.2: Turn-off voltage across a semiconductor measured at different time scales [21].

Apart from the voltage spike, there is also a current surge within the power converter during the transient switching period. Figure 4.3 shows a turn-on procedure of a semiconductor. The current surge is deduced during the turn-on process due to the parasitic capacitance of the transmission line.

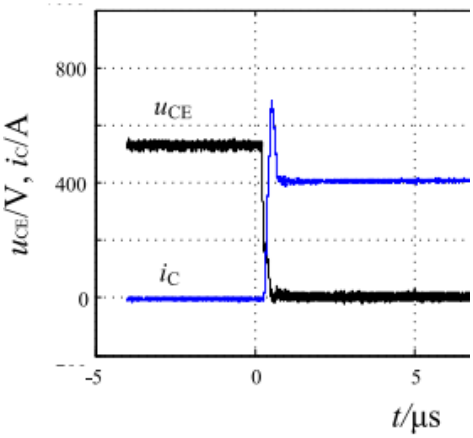

Figure 4.3: Turn-on current and voltage waveforms of a semiconductor considering the actual transmission line [21].

Transients during this process are complex and are difficult to study. Even the voltage and current spikes are mitigated using snubber circuits [22], sufficient voltage and current safe margin should be provided from the semiconductor SOA bound A and C in Figure 3.5, respectively. Thus, no more room is available for a well-designed and manufactured converter to enlarge its voltage and current ratings significantly.

4.1.2 Power Bound Limitation

The converter power limitation is majorly determined by the semiconductor power limitation. Specifically, the pulse length of the applied power pulse can change the maximum power losses (see the bound B in Figure 3.5). Usually, a longer conducting time (pulse width, which is determined by the PWM) leads to a reduced SOA area, as an SOA example shown in Figure 4.4. However, the use of PWM means a varying pulse width of the semiconductor and maximum pulse width is usually decided by the maximum duty cycle. At the same time, bound B has a thermal dependency, which means that the temperature should be kept below a limit (175°C for the example in Figure 4.4). The next section studies the limitations introduced by the converter heat.

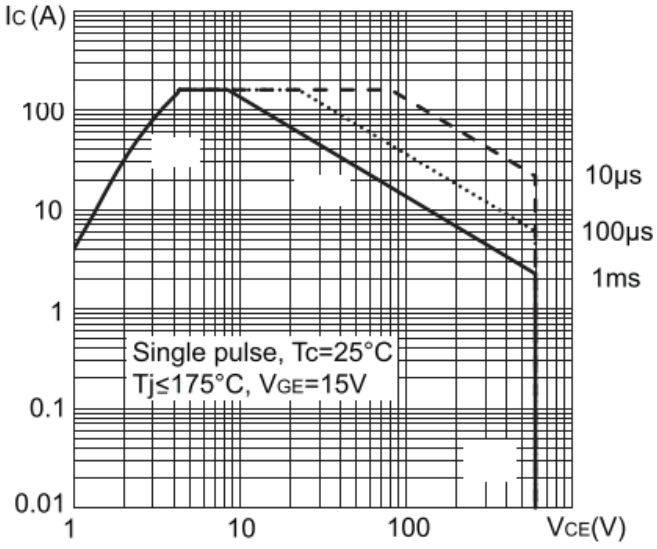

Figure 4.4: The relationship between the pulse width the bound B of the device SOA [19].

4.2 Thermal Design

To substantially utilise the power handling capability of the power converter (Figure 3.6, bound B), thermal design of the power converter should be considered. As converters have minimal overcurrent capability, the temperature should be kept below a minimum specified by the switch manufacturer. Otherwise, the power limit is severely reduced. A generic thermal resistance scheme for the semiconductor is shown in Figure 4.5, where Rth(j-c) is resistance from the junction to the case, Rth(c-h) is resistance the case to the heatsink, and Rth(h-a) is resistance from the heat sink to the ambient air.

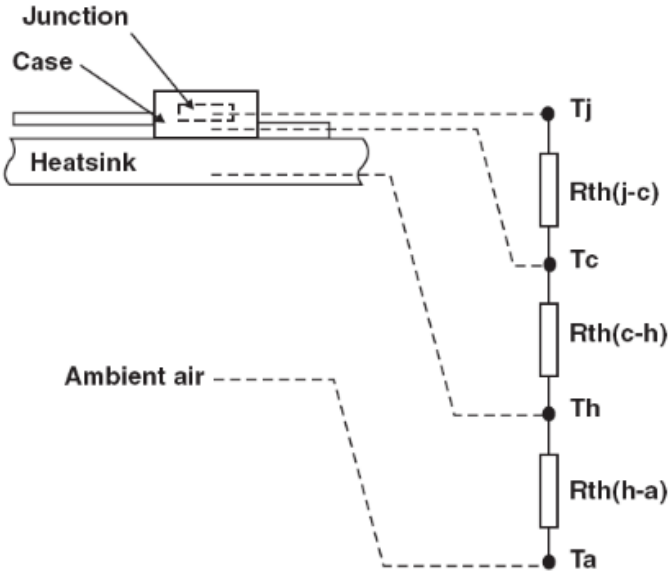

Figure 4.5: Thermal resistance scheme of a power semiconductor [19].

The thermal resistances are usually stated in the datasheets provided by the manufacture, where the overall resistance from the junction to the ambient (Rth(j-a)) consists Rth(j-c), Rth(c-h) and Rth(h-a), and helps to design an efficient heatsink. Power converter packages or heatsinks are designed to facilitate the thermal management of the device, as in [23], [24]. Also, forced cooling system with air or liquid could be used [25] to improve the heat transfer. All these measurements are aiming at reducing the thermal resistance between the junction (or case) and ambient of the power converter. A more detailed description of the thermal model can be found in [26].

Advanced techniques of packaging the semiconductors could be helpful to achieve the power converter with lower thermal resistance, higher current handling capability, smaller volume, better thermal management capability, as the three-dimensional packaging techniques given in [27] and [28]. Different thermal interface materials are evaluated in terms of performance and degradation, as presented in [29]. Figure 4.6 shows the heat sink examples for reducing the Rth(h-a), which is the main and effective approach to reduce the Rth(j-a) in terms of power converter design. Also, other heat sink types have been used for high cooling performance [30]–[32]. Therefore, the converter thermal behaviour could be analysed and assessed, as presented in [33].

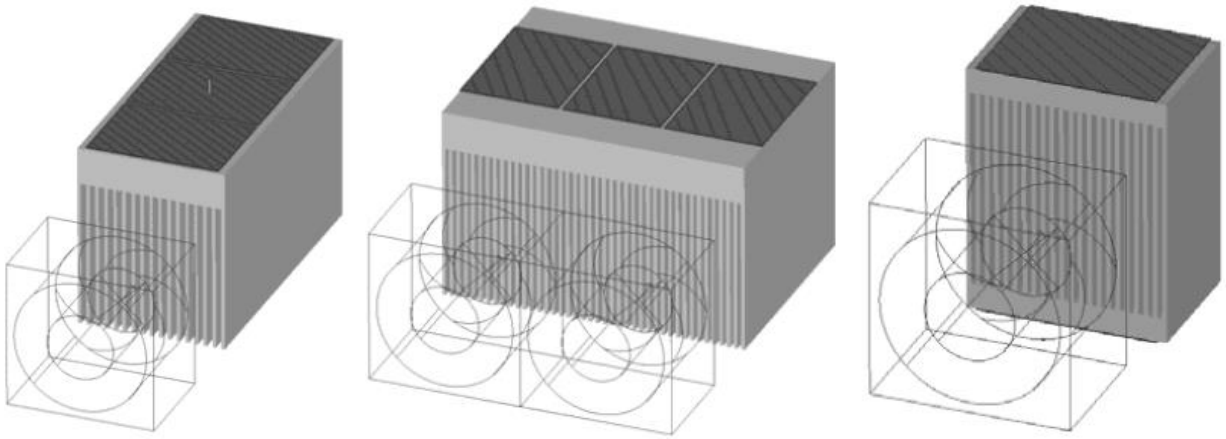

Figure 4.6: Various heat sinks with the optional fan schematics [25].

4.3 Converter Optimization

The limitations of power converters mainly lie on both the electric and thermal capacity of the semiconductors. During fault current provision scenarios, the converter operation points still cannot break the limits. Converter optimization and improvement could be considered to enlarge the converter capability, SSOA, but the gain might be quite small and always inside the semiconductor SOA.

5 Power Converter Control in Energy Generation Applications

5.1 Basic Control Structure and Targets

The control system has the mission to regulate the exchange of active power between the energy source and the grid keeping the current and voltage within the SSOA limits. Also, the grid side converter can provide other ancillary services such as voltage or reactive power support.

A generic power converter based energy generation system and control is illustrated in Figure 5.1, where the input side converter usually regulates the energy source including functions such as maximum power point tracking and the grid side converter mainly regulates the interaction with the grid including synchronization, power provision, fault ride through [34]. A transformer is used to match the voltage and provide galvanic insulation. Power converters should be interfaced with the grid using an inductive element, this element can be a dedicated inductance or the step-up transformer.

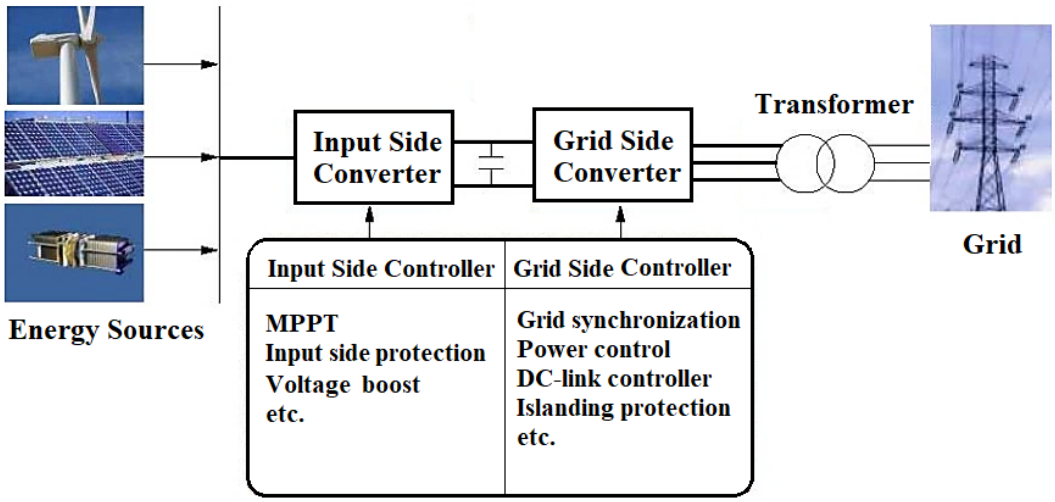

Figure 5.1: General structure of a power converter based generation system with its control [34].

5.2 Current Control

A popular approach to control the active and reactive power exchanged with the gird is the current control. In this approach, the ac current is regulated by controlling the voltage applied by the power converter. Figure 5.2 shows the typical PI controller based control scheme designed in the synchronous dq-frame. Depending on the reference axis, P and Q control can be achieved by manipulating the i_d and i_q components of the current.

Although these control structures are able to regulate the current under normal conditions, extra current limitation/saturation mechanism is needed when a fault occurs. The controller setpoint (reference command) is limited with respect to the calculated maximum current that the inverter can safely deliver [35]. With such design, the absolute value of the power semiconductor conducting current ($|i_{\max}| = \sqrt{i_d^{*2} + i_q^{*2}}$) can be controlled. This strategy allows the device to naturally limit the current without exceeding the converter SSOA and without producing a distorted current. Due to the current regulation scheme, the VSC is protected against overcurrent conditions. Other advantages of the current-mode control include robustness against variations in parameters of the VSC system and the ac system, superior dynamic performance, and higher control precision [3].

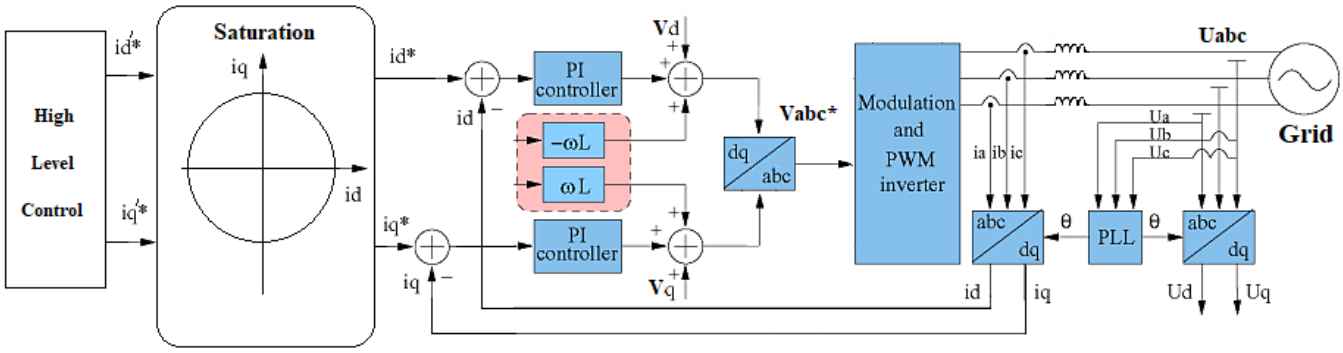

Figure 5.2: Control structure with current (for d and q axis) saturation block [4].

6 Grid Fault Ride-Through Requirements

When a fault occurs, power converters are programmed to provide maximum current respecting the SSOA limits. This can be achieved using the control scheme presented in Figure 5.2. Moreover, VSC converters allow controlling the current injected during a fault providing grid support during the fault [36], [37], the converter fault requirements are specified by the national grid codes [38]. This is known as Fault Ride Through (FRT).

A typical power converter connection FRT requirement characteristic is shown in Figure 6.1, where the converter should remain connected (white area) when the retained voltage is above V_{min} depending on the fault duration (t). In the case in which the voltage falls more than V_{min} or the fault last for longer, the converter may be isolated [39].

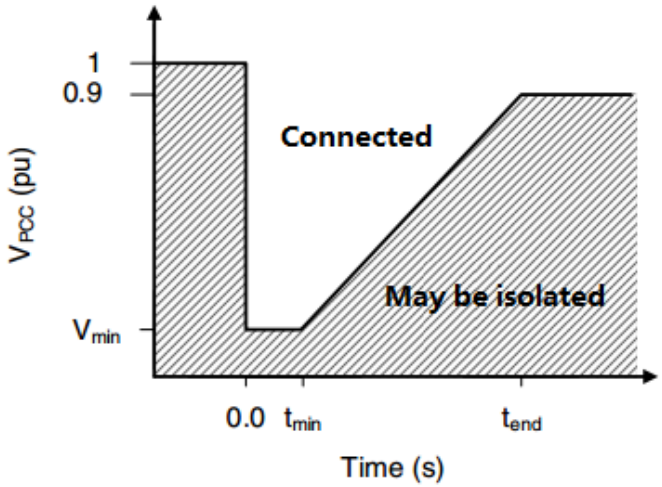

Figure 6.1: A typical example of a converter fault ride-through characteristic [39].

6.1 Grid Support

Given the controllability of the AC current during faults, converters are required not only to be connected but to support the grid. During the grid faults, power converter should be able to achieve a current injection into the grid [40]. Figure 6.2 shows a typical required reactive current curve during grid faults. The slope of the characteristic and the dead band can vary depending on the system operator requirements [41]. Some system operators might require active power injection instead of reactive.

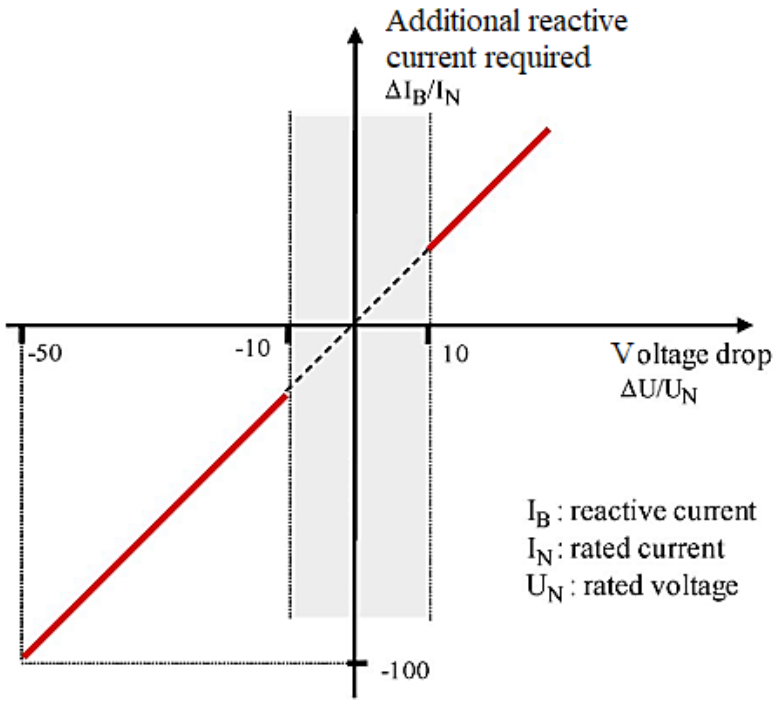

Figure 6.2: A typical required reactive current curve for voltage support [42].

In Ireland and GB, wind turbine converters must provide the maximum reactive current during a fault [43]. Figure 6.3 shows a specific reactive current provision characteristic, where the operational converter point is required to avoid falling into the shadow area. It should be noted that the reactive current provision has a minimum limitation, which is 0.9 pu in this example; whereas the maximum value mainly depends on the converter rating (operating area for converter) and protection margin.

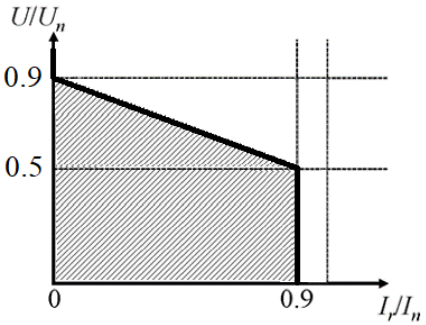

Figure 6.3: A typical example of converter fault ride-through fault current provision characteristic [43].

7 Cost Analysis of Power Converter Based Energy Generation Systems

This section analyses the cost aspects related to the fault current provision capability using power electronic converters. In general, power converters are designed for a maximum current around 1.1 pu, if more current wants to be provided, it will suppose an increase in cost as larger power switches will be required. It should be noted that the costs are highly depending on different economic conditions, environmental conditions, geographical factors, etc., whereas some data within this report vary dramatically.

7.1 Wind Power Generation System

Costs of the main components for the wind power generation systems, from various academic publications and technical reports, are given in Table 7.1, where the power converter, wind turbine, transformer and cable are considered, and the publishing year and reference type are presented. It could be seen that the general cost for power converters is about £0.81/kW but sources consulted by this project believe that the real cost is around £0.04-0.1k/kW (The used rate exchange currency is based on the data in 01-01-2017). The report's authors have checked industrial sources to verify this approximation.

Table 7.1: Cost Data of Wind Power Generation Systems.

Ref. / **Item**	[44]	[45]	[46]	[47]	[48]	[49]	[50]	[51]
Power Converter	$1k/kW	$0.75k/kW	-	-	£0.06k/kW	€1k/kW	-	-
Wind Turbine electric components (general)	$3.5k/kW	$2k/kW	€1.5k/kW	$1k/kW	-	-	$1.4k/kW	-
Transformer	-	-	€0.085k/kW	-	€0.005k/kW	-	-	-
Cable	-	-	€0.3k/m	-	£0.67k/m	€2.1k/m	-	€0.0238k/m
Remarks	-	One dc wind turbine is considered. Converter is considered as 10, 15 kW.	A 5 MW turbine is considered; Transformer is 20/150 kV. Cable is from offshore to shore.	Wind turbines with rotors larger than 95m is considered. Average cost is presented.	Single wind turbine ac/dc and dc/ac converter are considered. A 200MW transformer is considered. A 30–36 kVac cable with 1kA is considered.	An MMC type power converter is considered. One 155kV three-phase cable (800 mm^2 incl. installation) is considered.	An average value of six turbines is presented.	Cables with 12/20 kV and 592A.
Ref Type (J/C/R)	J	J	C	R	J	C	J	J
Ref Year	2014	2015	2015	2016	2015	2019	2009	2016

Ref Type (J/C/R): J: Journal; C: Conference Proceeding; R: Report

A cost breakdown for the off-shore wind farm system has been reported in [47], as shown in Figure 7.1. The main cost components of offshore wind farms are the turbines (including towers), the foundations and grid connection to shore. It can be observed that the costs related to the electrical infrastructure include transmission system (high voltage AC or DC system, where a typical configuration is two or more offshore substations) and electrical array, which counts for 16% of all.

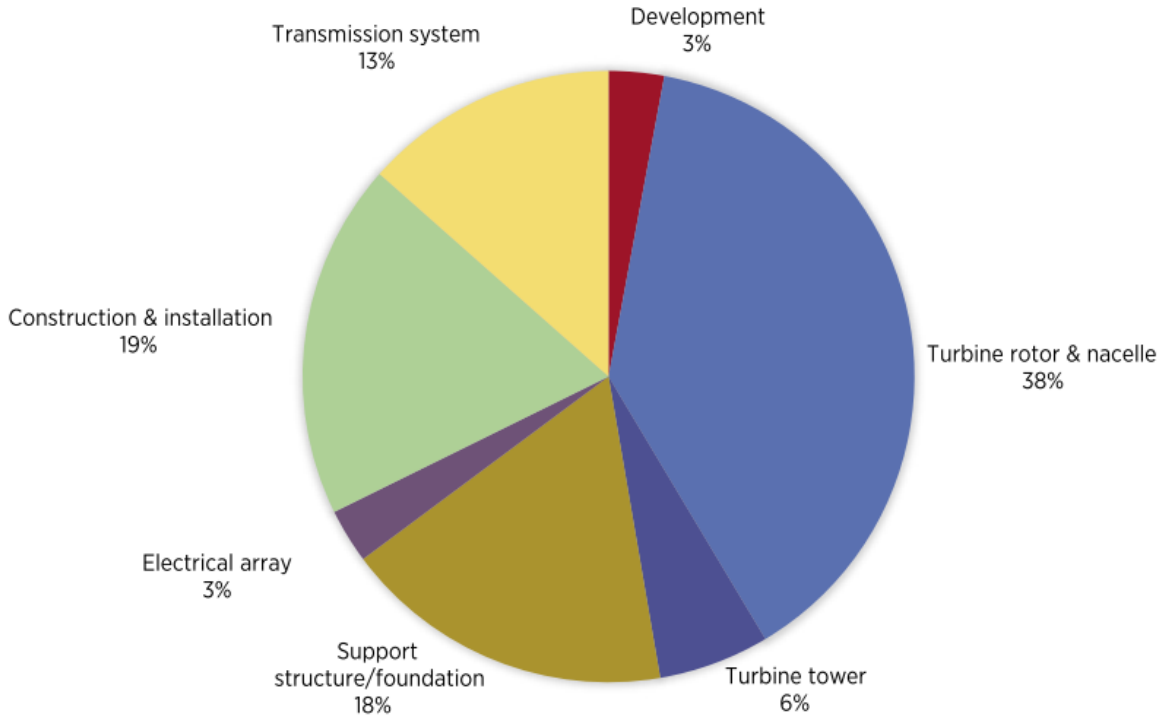

Figure 7.1: Cost breakdown for an offshore wind farm generation system in [47].

Another investigation reports similar data, with the electrical infrastructure counts for about 10% of the overall cost [52]. Moreover, based on the presented data in [53], the cost breakdown of the onshore and offshore wind generation systems are shown in Figure 7.2. It can be seen that the electrical infrastructure costs 9% for the onshore wind generation system while the offshore infrastructure is more expensive due to the longer distance between the wind farm and the point of connection.

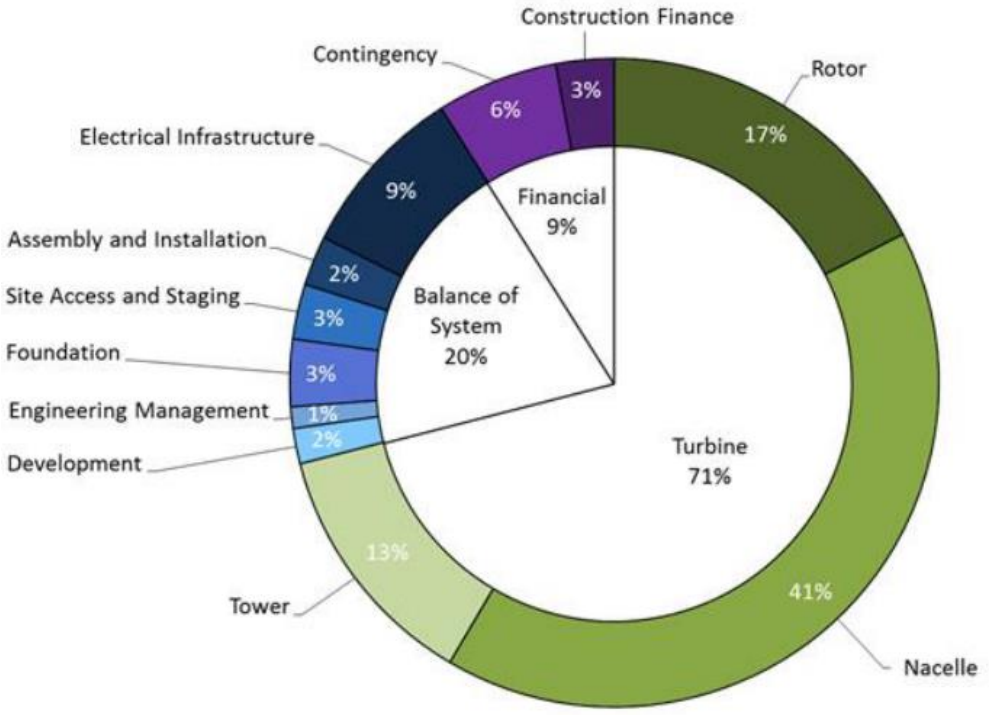

(a) Capital expenditures for the on-shore wind generation project.

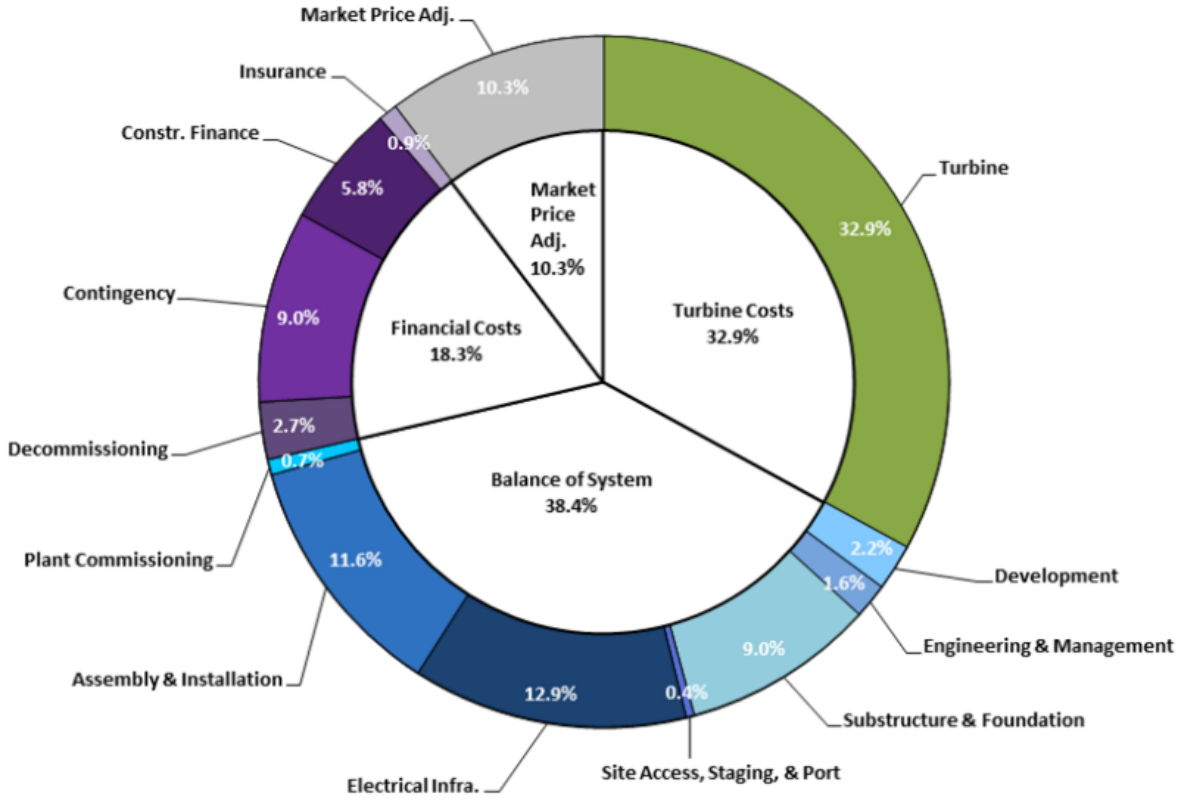

(b) Capital expenditures for the offshore wind generation project.

Figure 7.2: Cost breakdown for the wind farm generation system in [53].

Regarding the cost of the power electronics device, some studies show that the cost is around 3.5% of the overall onshore wind power generation system [54]. The detailed cost breakdown information is shown in Figure 7.3. Also, the same study identifies the price of the converter for an offshore turbine around 5%.

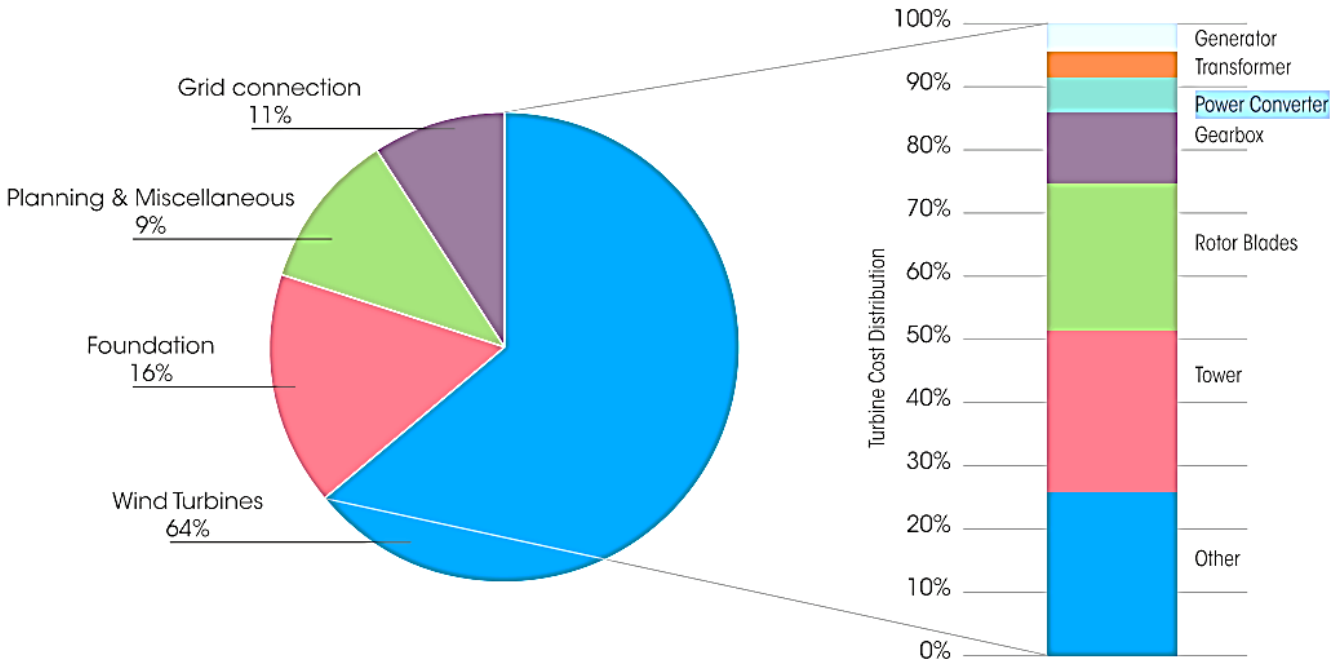

Figure 7.3: Component costs for the wind generation system in [54].

There is an apparent price mismatch between the power electronics prices found in the literature and the ones found in IRENA reports. Literature report prices between £0.06k/kW £1k/kW while the IRENA literature reports costs around 3-4% for Onshore wind turbines and 5% for offshore. After consulting several industrial sources, they agreed with the relative cost provided by IRENA.

7.2 Solar Power Generation System

The studied costs for the solar power generation systems are given in Table 7.2, where the power converter and solar panel are considered, and the publishing year and reference type are presented.

Table 7.2: Cost Data of Solar Power Generation Systems.

Ref. / Item	[55]	[44]	[45]	[47]	[56]	[57]
Power Converter	-	$1k/kW	$0.75k/kW	$0.2k/kW	€0.08k/kW	$0.14k/kW
Solar Panel	$1.6k/kW	$6.5k/kW	$2.8k/kW	$0.62k/kW	€0.38k/kW	$0.47k/kW
Remarks	All monetary values are in Australian dollars.	-	Converter is considered as 10, 15 kW. PV panel is sized from 20 to 40 kW.	Weighted average country level module prices are considered and average value is presented.	Average values of the statistics in 2016 are presented.	Average cost for the power converter; Ex-factory price for Tier-1 modules.
Ref Type (J/C/R)	J	J	J	R	J	R
Ref Year	2015	2014	2015	2016	2017	2018

Ref Type (J/C/R): J: Journal; C: Conference Proceeding; R: Report

It is possible for the power converter cost to be lower than £0.81k/kW but a large variation is presented in the literature. However, data from [47] and [57] could be more reliable as they are updated journal articles. The cost of different components in percentage for the solar generation systems is shown in Figure 7.4. The power electronic converter (inverter) varies between 3% to 8% approximately.

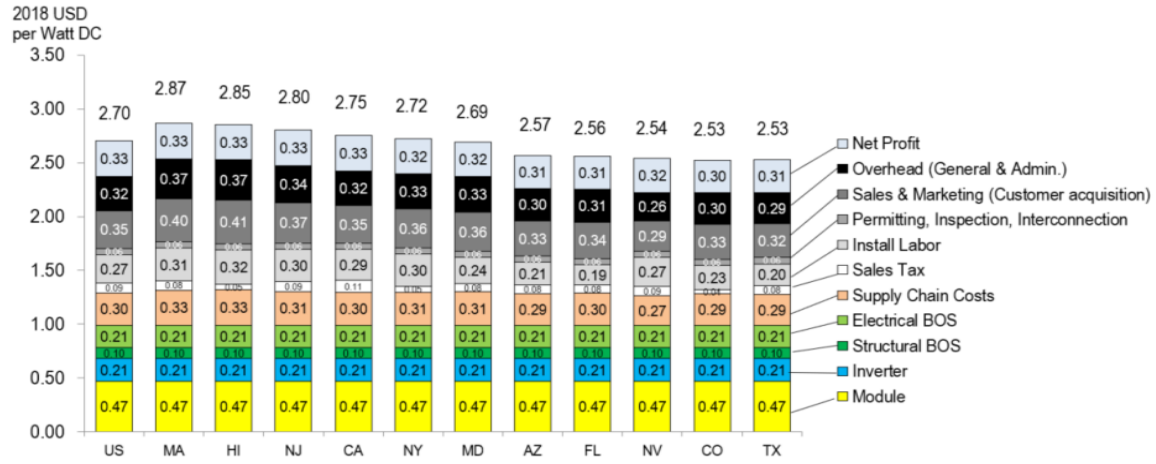

(a) 6.2kW residential solar generation system cost (2018 $/W).

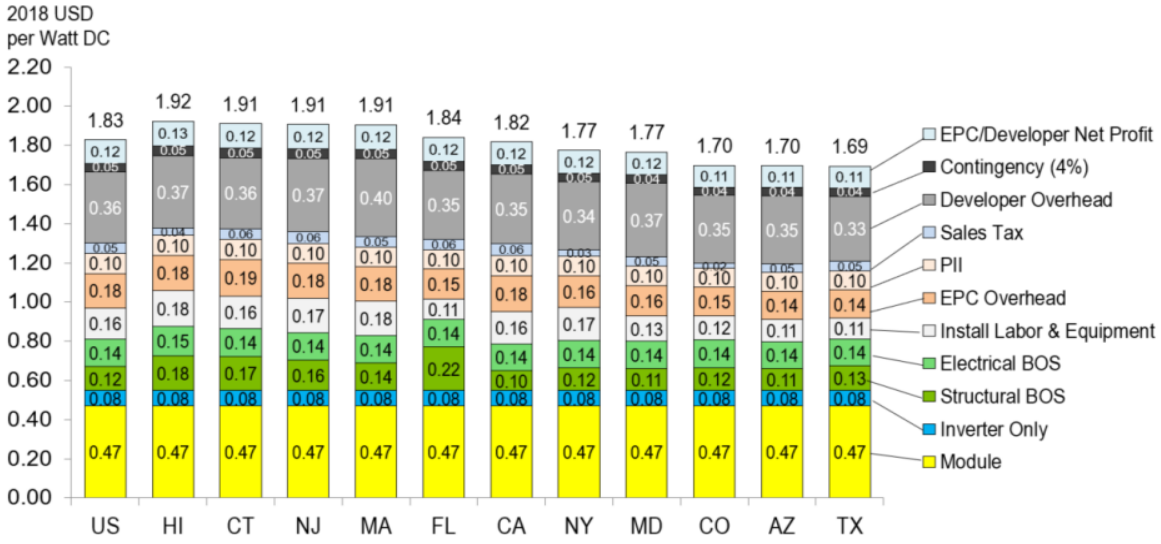

(b) 200kW commercial solar generation system cost (2018 $/W).

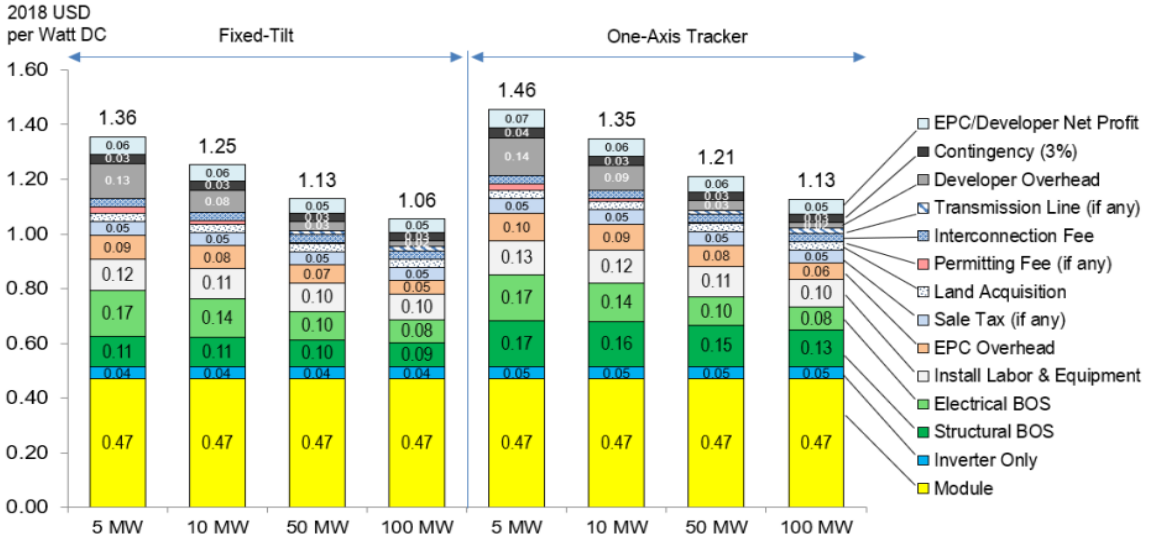

(c) utility-scale solar generation system cost (2018 $/W).

Figure 7.4: Component costs for the solar generation system in [57].

Another study reported in [47] provides the cost data, whereas the related percentages are shown in Figure 7.5.

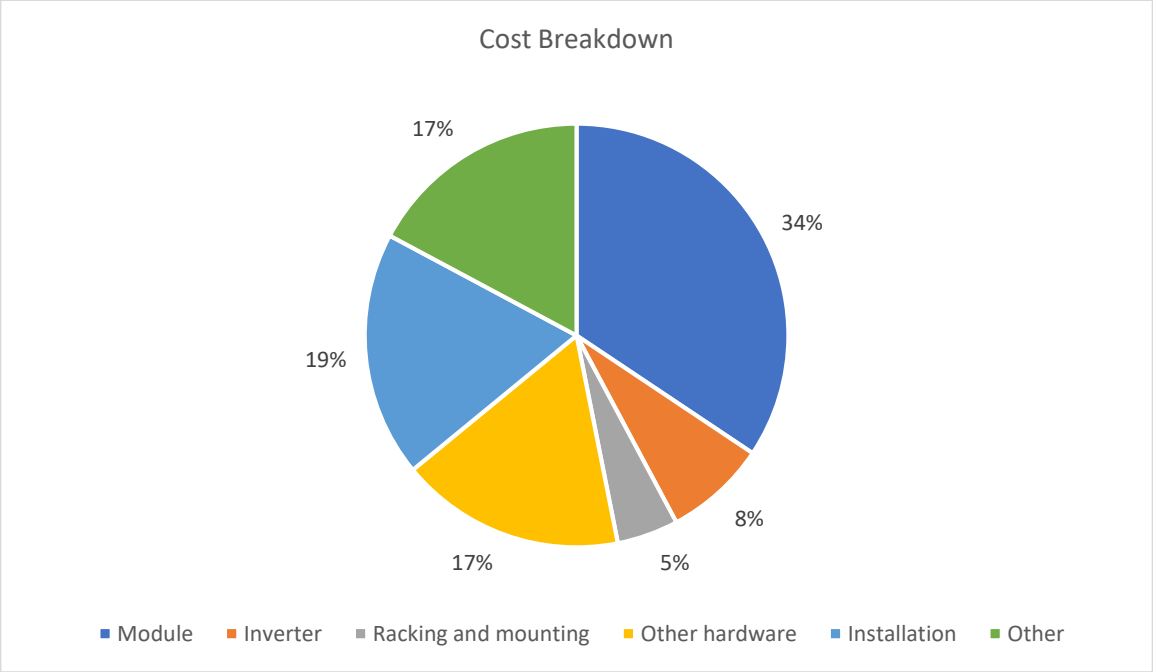

Figure 7.5: Cost breakdown for the solar generation system in [47].

From this result, the power inverter costs 8% of the overall cost for solar systems. However, it should be noted that this result does not consider soft costs such as those for operation, maintenance, etc.

7.3 HVDC System

Costs of the HVDC systems are shown in Table 7.3, where the power converter, wind turbine, transformer, transformer and cable are considered, and the publishing year and reference type are presented.

Table 7.3: Cost Data of HVDC systems.

Ref. / **Item**	[48]	[49]	[58]	[59]	[60]	[61]
Power Converter	£0.165k/kW	€1k/kW	£0.24k/kW	€0.123k/kW	JPY14k/kW	€0.12k/kW
Transformer	€0.005k/kW	-	£0.05k/kW	€0.05k/kW	-	-
Cable	£0.178k/m	€2.6k/m	£0.9k/m	-	-	-
Remarks	A dc converter is priced; 200MW transformer is considered. A 30kVdc cable with 1kA is considered.	System voltage is rated at +/- 320kVdc with 900MW power.	A 200MW offshore station is considered.	A 200MW offshore station is used for calculation.	A 500kV dc system is considered.	100MW and 60km
Ref Type (J/C/R)	J	C	C	C	C	J
Ref Year	2015	2019	2016	2019	2019	2006

Ref Type (J/C/R): J: Journal; C: Conference Proceeding; R: Report

The cost of an HVDC transmission system depends, especially, on a large number of factors (such as power capacity to be transmitted, type of transmission medium, environmental conditions and other safety, regulatory requirements etc.). A typical cost structure is shown in Figure 7.6, where the power converter cost is 33% of the overall, whereas the DC transmission cable cost is 34% of the total [62].

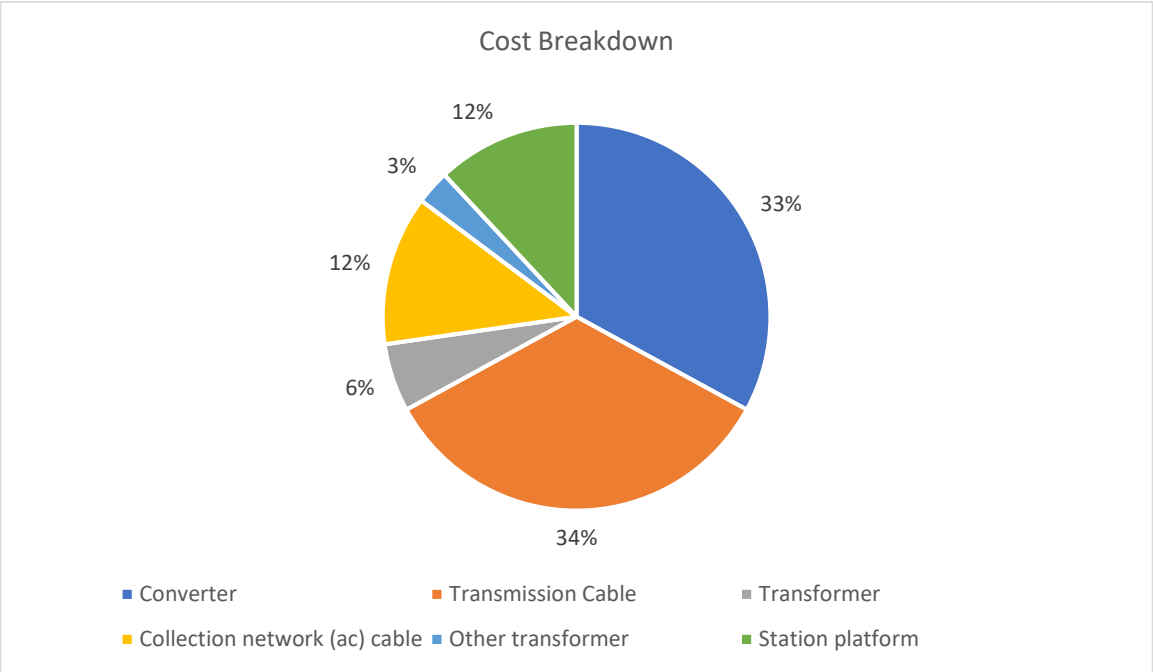

Figure 7.6: Cost breakdown for the HVDC system in [62].

Another research claims that the converter station and transmission line count for 31%-39% and 33%-44% of the overall HVDC system cost respectively [63].

7.4 Summary

Figure 7.7 shows the unit costs of the power converter in wind and solar power generation, and HVDC applications. And Figure 7.8 shows the cost variations over the last six years. These data are calculated based on the average values in Table 7.1, Table 7.2 and Table 7.3.

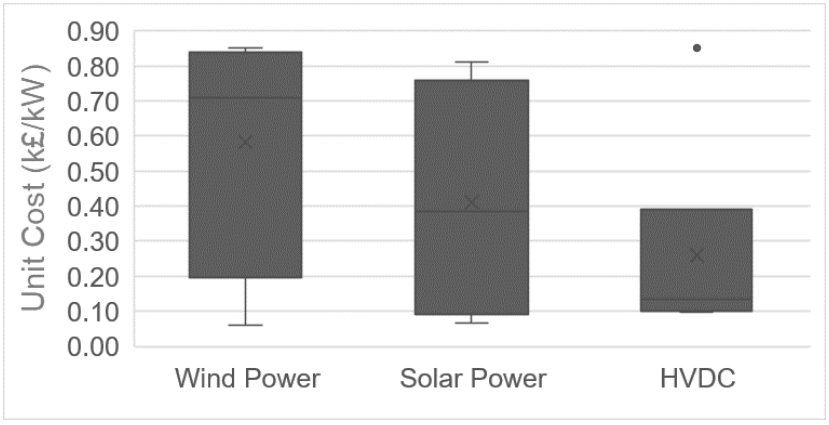

*** Rate exchange currency is based on the data in 01-01-2017.**

Figure 7.7: Power converter cost in different applications.

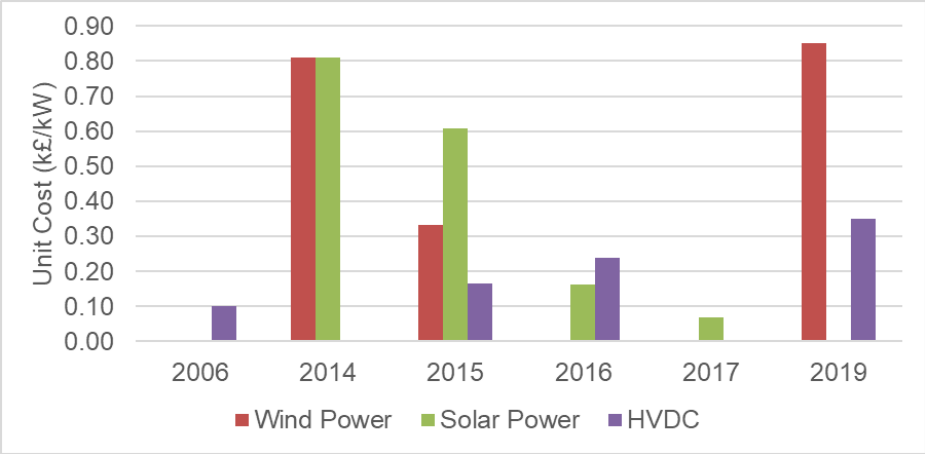

*** Rate exchange currency is based on the data in 01-01-2017.**

Figure 7.8: Power converter cost variation with years.

There is not a precise cost estimation for power electronics for wind and solar generation and HVDC but looking at the present literature and discussion with manufacturers we believe that the cost for the power electronics for wind applications is around £0.04-0.1k/kW and represents between 3-5% of the total cost of the wind farm. For HVDC and solar applications, the price is also around £0.057-0.097k/kW.

8 Appendix A: Basic Definitions

Diode and Thyristors:

A diode is a two-terminal electronic component that conducts current primarily in one direction. When the voltage across the device is positive, the diode starts to conduct and the conduction ends when the current crosses zero again. A thyristor is a three-terminal switch that has shared properties with the diode but the conduction starts when an electrical signal is applied to the gate.

IGBT:

An Insulated Gate Bipolar Transistor is a three-terminal forced commutation, usually is used for high power low switching frequency applications. This switch can be turned on an off applying an electrical signal in the gate of the device. It is the most common switch used in renewable power applications.

MOSFET:

A Metal-Oxide-Semiconductor Field Effect or MOSFET is a three-terminal forced commutation, usually is used for low-to-medium power and high switching frequency applications. This switch can be turned on and off applying an electrical signal in the gate of the switch. It is the most common switch used in renewable power applications.

Power Converter, Converter, Power Electronics or Convertor:

A power converter is a static electrical device that allows the conversion of the electrical energy from one form to another. A power converter that converts DC energy in AC is called inverter and a power converter that converts AC energy in DC is called rectifier. Power converters are composed by electrical components called switches, being the most used the diodes, thyristors, MOSFET or IGBT.

PWM modulation:

PWM or Pulse Width Modulation is a high-frequency modulation technique used in forced commutated converters to generate voltages at low frequency when a discrete DC voltage is available. This technique is the most common method to create an AC voltage in VSC.

Voltage Source Converter (VSC):

A VSC or Voltage Source Converter is a power converter that behaves like an AC voltage source. This is the most common kind of power converter for grid-connected applications. For applications in the range of the MW, the most used power converters are the two-level.

Fault ride-through:

The Fault ride-through is the capability of an electric generator or a power converter to stay connected when the electrical voltage is disturbed such as a voltage sag or an overvoltage.

qd-frame:

The qd-frame is a frame used in electrical engineering where a three-phase sinusoidal signal is simplified into two constant quantities. The transformation that allows transforming any three-phase signal into the qd-frame is called the Park transformation. This transformation needs an angle as a reference. Three-phase inverter control systems require a Phase Locked Loop to provide this angle.

PLL:

A PLL is a control system that generates an output signal related to the phase of the input signal. In three phase converters, this element is used to estimate the grid angle at the converter point of connection. Usually, a PLL is composed of a PI that determines the grid frequency and an integrator that determines the grid angle.

Wind Energy Conversion System:

A Wind Energy Conversion System or WECS or Wind Turbine is an electromechanical device that transforms the wind energy in electrical energy. The components of a standard wind turbine drive train are the turbine, the gearbox, the generator, the converter and the transformer.

Energy Storage System:

Energy Storage System or ESS is devices that store energy in different forms and it is exchanged with the grid when required. Standard ESS for power system applications are batteries, flying wheels or supercapacitors.

9 Appendix B: Current Limitation Considering Junction Temperature

An active approach for semiconductor operating point control and dynamic thermal regulation is proposed in [64], where a new controller is added to the current loop to modulate the current limits. The propose control loop is shown in

Figure 9.1, with the reference values being semiconductors junction temperature, which is treated as an operational constraint. This is a concept under research and it is not standard practice.

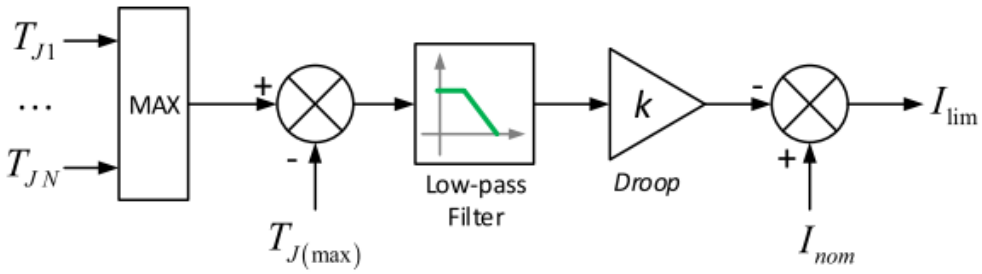

Figure 9.1: Proposed control scheme for the current limit [64].

The basic mechanism is that an increased junction temperature will lead to decreased absolute current references, whereas absolute current references increase when the junction temperature is in low range. Besides, stability analysis for such a current manipulation process is required. Figure 9.2 shows a transient behaviour under a 100ms phase-to-ground fault at 6s, with the proposed control method.

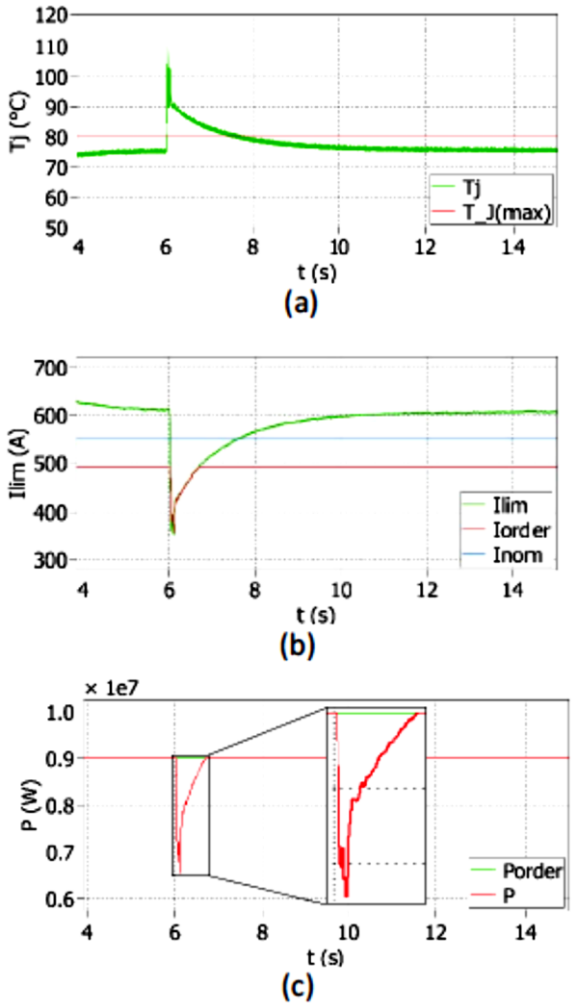

Figure 9.2: Response of the converter in transient phase with dynamic current limits: (a) junction temperature limits, (b) current limit value, and (c) active power [64].

The high fault current magnitude causes an increase in the temperature which in turn leads to a decrease in the current order and the injected power. After the fault is cleared and the temperature starts to decrease, the current limit increases accordingly. Therefore, the controller is able to deliver additional response by taking into account the operating point (within SOA) of the semiconductors and exploiting the additional thermal headroom available.

10 Appendix C: Costs of Energy Storage Elements

Ref. / Item	[65] (€/kWh)	[45] ($/kWh)	[66] (€/kWh)	[67] ($/kWh)	[68] ($/kWh)	[69] ($/kWh)	[70] ($/kWh)	[71] ($/kWh)
Lead Acid Battery	618	160	380	-	-	100-300	-	-
Li-ion Battery	795	-	915	600-2500	500-2500	300-2500	400	300
VRB	298	-	-	-	460-1600	-	-	-
Super-capacitor	-	-	-	500-1500	-	-	2500	-
Remarks	Average costs are given for the typical size of each technology.	A 6V battery (Surrette 6CS25P) with a nominal capacity of 1156 Ah and with the lifetime throughput of 9645 kWh is selected from the HOMER data base. 8-32 units are considered.	-	-	-	-	-	-
Ref Type (J/C/R)	J	J	J	J	J	J	J	J
Ref Year	2015	2015	2016	2016	2017	2018	2018	2017

Ref Type (J/C/R): J: Journal; C: Conference Proceeding; R: Report

11 References

[1] B. W. Williams, *Power Electronics: Devices, Drivers, Applications, and Passive Components*. Glasgow, 2006.

[2] L. Franquelo, J. Rodriguez, J. Leon, S. Kouro, R. Portillo, and M. Prats, "The age of multilevel converters arrives," *IEEE Ind. Electron. Mag.*, vol. 2, no. 2, pp. 28–39, Jun. 2008, doi: 10.1109/MIE.2008.923519.

[3] A. Yazdani and R. Iravani, *Voltage-Sourced Converters in Power Systems: Modeling, Control, and Applications*. Hoboken: John Wiley & Sons, Inc., 2010.

[4] N. Flourentzou, V. G. Agelidis, and G. D. Demetriades, "VSC-based HVDC power transmission systems: An overview," *IEEE Trans. Power Electron.*, vol. 24, no. 3, pp. 592–602, 2009, doi: 10.1109/TPEL.2008.2008441.

[5] S. Kouro *et al.*, "Recent Advances and Industrial Applications of Multilevel Converters," *IEEE Trans. Ind. Electron.*, vol. 57, no. 8, pp. 2553–2580, Aug. 2010, doi: 10.1109/TIE.2010.2049719.

[6] M. A. Perez, S. Bernet, J. Rodriguez, S. Kouro, and R. Lizana, "Circuit Topologies, Modeling, Control Schemes, and Applications of Modular Multilevel Converters," *IEEE Trans. Power Electron.*, vol. 30, no. 1, pp. 4–17, Jan. 2015, doi: 10.1109/TPEL.2014.2310127.

[7] J. L. Kirtley, M. S. El Moursi, and W. Xiao, "Fault ride through capability for grid interfacing large scale PV power plants," *IET Gener. Transm. Distrib.*, vol. 7, no. 9, pp. 1027–1036, Sep. 2013, doi: 10.1049/iet-gtd.2013.0154.

[8] E. H. Camm *et al.*, "Characteristics of wind turbine generators for wind power plants," in *2009 IEEE Power & Energy Society General Meeting*, 2009, pp. 1–5, doi: 10.1109/PES.2009.5275330.

[9] E. Muljadi, N. Samaan, V. Gevorgian, J. Li, and S. Pasupulati, "Short circuit current contribution for different wind turbine generator types," *IEEE PES Gen. Meet. PES 2010*, pp. 1–8, 2010, doi: 10.1109/PES.2010.5589677.

[10] M. Vilathgamuwa, D. Nayanasiri, and S. Gamini, *Power Electronics for Photovoltaic Power Systems*, vol. 5, no. 2. 2015.

[11] B. Gemmell, J. Dorn, D. Retzmann, and D. Soerangr, "Prospects of multilevel VSC technologies for power transmission," in *2008 IEEE/PES Transmission and Distribution Conference and Exposition*, 2008, pp. 1–16, doi: 10.1109/TDC.2008.4517192.

[12] R. J. Dávalos M, J. M. Ramírez A, and R. Tapia, "Multi-step static VAR compensators analysis," *Proc. IEEE Power Eng. Soc. Transm. Distrib. Conf.*, vol. 3, no. SUMMER, pp. 1451–1456, 2002, doi: 10.1109/pess.2002.1043628.

[13] Y. Zhao, Q. Liang, S. Dong, and Q. Zhao, "Research on three-level static synchronous compensator," in *The 2nd International Symposium on Power Electronics for Distributed Generation Systems*, 2010, no. 59, pp. 639–644, doi: 10.1109/PEDG.2010.5545911.

[14] B. Singh, R. Saha, A. Chandra, and K. Al-Haddad, "Static synchronous compensators (STATCOM): A review," *IET Power Electron.*, vol. 2, no. 4, pp. 297–324, 2009, doi: 10.1049/iet-pel.2008.0034.

[15] Z. Yang, C. Shen, L. Zhang, M. L. Crow, and S. Atcitty, "Integration of a StatCom and battery energy storage," *Proc. IEEE Power Eng. Soc. Transm. Distrib. Conf.*, vol. 3, no. SUMMER, p. 1798, 2001, doi: 10.1109/mper.2001.4311386.

[16] I. Batarseh and A. Harb, *Power Electronics: Circuit Analysis and Design*, 2nd Editio. Springer Nature, 2018.

[17] J . Schoiswohl, "Application Note: Linear Mode Operat ion and Safe Operat ing Diagram of Power-MOSFETs," Munich, 2017.

[18] R. Electronics, "IGBT Application Note (R07AN0001EJ0410)," 2018.

[19] STMicroelectronics, "Application note (AN4544): IGBT datasheet tutorial Introduction," 2014.

[20] G. Zou, Z. Zhao, L. Yuan, X. Wang, and T. Lu, "Optimal design of the back-to-back IGBT-based converter with the concept of systematic safe operating area," in *2011 International Conference on Electrical Machines and Systems*, 2011, pp. 1–5, doi: 10.1109/ICEMS.2011.6073729.

[21] Z. Zhao, D. Tan, and K. Li, "Transient Behaviors of Multiscale Megawatt Power Electronics Systems—Part I: Characteristics and Analysis," *IEEE J. Emerg. Sel. Top. Power Electron.*, vol. 7, no. 1, pp. 7–17, Mar. 2019, doi: 10.1109/JESTPE.2019.2894424.

[22] L. Yuan, Z. Zhao, M. Eltawil, R. Yi, and H. Bai, "Performance Evaluation of Switch Devices Equipped in High-Power Three-Level Inverters," *IEEE Trans. Ind. Electron.*, vol. 54, no. 6, pp. 2993–3000, Dec. 2007, doi: 10.1109/TIE.2007.906999.

[23] P. Vinciarelli, M. B. Lafleur, C. I. Mccauley, and P. V. Starenas, "Power Converter Package and Thermal Management," 2008.

[24] R. Ye and A. J. Zhang, "Power Converter Package with Enhanced Thermal Management," 2004.

[25] U. Drofenik, G. Laimer, J. W. Kolar, O. Strategy, and H. Power, "Theoretical Converter Power Density Limits for Forced Convection Cooling," *Proc. Int. PCIM Eur. 2005 Conf.*, no. 4, pp. 608–619, 2005.

[26] A. S. Bahman, K. Ma, and F. Blaabjerg, "A Lumped Thermal Model Including Thermal Coupling and Thermal Boundary Conditions for High-Power IGBT Modules," *IEEE Trans. Power Electron.*, vol. 33, no. 3, pp. 2518–

2530, Mar. 2018, doi: 10.1109/TPEL.2017.2694548.
[27] J. N. Calata, J. G. Bai, X. Liu, S. Wen, and G. Q. Lu, “Three-dimensional packaging for power semiconductor devices and modules,” *IEEE Trans. Adv. Packag.*, vol. 28, no. 3, pp. 404–412, 2005, doi: 10.1109/TADVP.2005.852837.
[28] E. Vagnon, P. O. Jeannin, J. C. Crébier, and Y. Avenas, “A bus-bar-like power module based on three-dimensional power-chip-on-chip hybrid integration,” *IEEE Trans. Ind. Appl.*, vol. 46, no. 5, pp. 2046–2055, 2010, doi: 10.1109/TIA.2010.2057401.
[29] T. Semenic, A. Bhunia, N. Gollhardt, G. Morris, and R. Lukaszewski, “Low thermal resistance thermal pad for power converter modules,” in *2017 IEEE 12th International Conference on Power Electronics and Drive Systems (PEDS)*, 2017, vol. 2017-Decem, no. December, pp. 453–455, doi: 10.1109/PEDS.2017.8289121.
[30] T. L. Anderson, H. Dk, and H. B. Moller, “HEAT SINK FOR COOLING OF POWER SEMCONDUCTOR MODULES,” 2017.
[31] I. E. Parker *et al.*, “TRANSFORMER-BASED POWER CONVERTERS WITH 3D PRINTED MCROCHANNEL HEAT SNK,” 2016.
[32] J. N. Husser and E. Dixler, “HEAT SNK DEVICE FOR POWER MODULES OF POWER CONVERTER ASSEMBLY,” 2016.
[33] P. Cova *et al.*, “Thermal optimization of water heat sink for power converters with tight thermal constraints,” *Microelectron. Reliab.*, vol. 53, no. 9–11, pp. 1760–1765, 2013, doi: 10.1016/j.microrel.2013.07.035.
[34] A. Timbus, M. Liserre, R. Teodorescu, P. Rodriguez, and F. Blaabjerg, “Evaluation of Current Controllers for Distributed Power Generation Systems,” *IEEE Trans. Power Electron.*, vol. 24, no. 3, pp. 654–664, Mar. 2009, doi: 10.1109/TPEL.2009.2012527.
[35] M. Castilla, J. Miret, A. Camacho, J. Matas, and L. G. De Vicuña, “Voltage support control strategies for static synchronous compensators under unbalanced voltage sags,” *IEEE Trans. Ind. Electron.*, vol. 61, no. 2, pp. 808–820, 2014, doi: 10.1109/TIE.2013.2257141.
[36] H. Urdal, R. Ierna, J. Zhu, C. Ivanov, A. Dahresobh, and D. Rostom, “System strength considerations in a converter dominated power system,” *IET Renew. Power Gener.*, vol. 9, no. 1, pp. 10–17, 2015, doi: 10.1049/iet-rpg.2014.0199.
[37] A. Cabrera-Tobar, E. Bullich-Massagué, M. Aragüés-Peñalba, and O. Gomis-Bellmunt, “Review of advanced grid requirements for the integration of large scale photovoltaic power plants in the transmission system,” *Renew. Sustain. Energy Rev.*, vol. 62, pp. 971–987, 2016, doi: 10.1016/j.rser.2016.05.044.
[38] L. S. Xavier, W. C. S. Amorim, A. F. Cupertino, V. F. Mendes, W. C. do Boaventura, and H. A. Pereira, “Power converters for battery energy storage systems connected to medium voltage systems: a comprehensive review,” *BMC Energy*, vol. 1, no. 1, p. 7, Dec. 2019, doi: 10.1186/s42500-019-0006-5.
[39] C. Abbey and G. Joos, “Effect of low voltage ride through (LVRT) characteristic on voltage stability,” *2005 IEEE Power Eng. Soc. Gen. Meet.*, vol. 2, pp. 1901–1907, 2005, doi: 10.1109/pes.2005.1489659.
[40] O. A. Giddani, G. P. Adam, O. Anaya-Lara, G. Burt, and K. L. Lo, “Control strategies of VSC-HVDC transmission system for wind power integration to meet GB grid code requirements,” in *SPEEDAM 2010*, 2010, pp. 385–390, doi: 10.1109/SPEEDAM.2010.5542237.
[41] C. Rahmann, H.-J. Haubrich, A. Moser, R. Palma-Behnke, L. Vargas, and M. B. C. Salles, “Justified Fault-Ride-Through Requirements for Wind Turbines in Power Systems,” *IEEE Trans. Power Syst.*, vol. 26, no. 3, pp. 1555–1563, Aug. 2011, doi: 10.1109/TPWRS.2010.2093546.
[42] C. Rahmann, H. J. Haubrich, A. Moser, R. Palma-Behnke, L. Vargas, and M. B. C. Salles, “Justified fault-ride-through requirements for wind turbines in power systems,” *IEEE Trans. Power Syst.*, vol. 26, no. 3, pp. 1555–1563, 2011, doi: 10.1109/TPWRS.2010.2093546.
[43] D. Xie, Z. Xu, L. Yang, J. Ostergaard, Y. Xue, and K. P. Wong, “A Comprehensive LVRT Control Strategy for DFIG Wind Turbines with Enhanced Reactive Power Support,” *IEEE Trans. Power Syst.*, vol. 28, no. 3, pp. 3302–3310, 2013, doi: 10.1109/TPWRS.2013.2240707.
[44] Y. Kalinci, A. Hepbasli, and I. Dincer, “Techno-economic analysis of a stand-alone hybrid renewable energy system with hydrogen production and storage options,” *Int. J. Hydrogen Energy*, vol. 40, no. 24, pp. 7652–7664, Jun. 2015, doi: 10.1016/j.ijhydene.2014.10.147.
[45] S. Ghaem Sigarchian, R. Paleta, A. Malmquist, and A. Pina, “Feasibility study of using a biogas engine as backup in a decentralized hybrid (PV/wind/battery) power generation system – Case study Kenya,” *Energy*, vol. 90, pp. 1830–1841, Oct. 2015, doi: 10.1016/j.energy.2015.07.008.
[46] M. Beccali, J. Galletto, L. Noto, and R. Provenza, “Assessment of the technical and economic potential of offshore wind energy via a GIS application: A case study for the Sicily Region according to Italian laws and incentive frameworks,” in *2015 International Conference on Renewable Energy Research and Applications (ICRERA)*, 2015, vol. 5, pp. 1342–1347, doi: 10.1109/ICRERA.2015.7418627.
[47] IRENA, “The Power to Change: Solar and Wind Cost Reduction Potential to 2025,” 2016.

[48] P. Lakshmanan, J. Liang, and N. Jenkins, “Assessment of collection systems for HVDC connected offshore wind farms,” *Electr. Power Syst. Res.*, vol. 129, pp. 75–82, Dec. 2015, doi: 10.1016/j.epsr.2015.07.015.
[49] M. Hoffmann, C. Rathke, A. Menze, N. G. A. Hemdan, and M. Kurrat, “Parallel Operation of HVDC DRU and VSC Converters for Offshore Wind Farm Connection: Technical and Economic Feasibility,” in *15th IET International Conference on AC and DC Power Transmission (ACDC 2019)*, 2019, vol. 2019, no. CP751, pp. 57 (6 pp.)-57 (6 pp.), doi: 10.1049/cp.2019.0057.
[50] Li Wang, Tai-Her Yeh, We-Jen Lee, and Zhe Chen, “Benefit Evaluation of Wind Turbine Generators in Wind Farms Using Capacity-Factor Analysis and Economic-Cost Methods,” *IEEE Trans. Power Syst.*, vol. 24, no. 2, pp. 692–704, May 2009, doi: 10.1109/TPWRS.2009.2016519.
[51] A. Cerveira, A. F. de Sousa, E. J. S. Pires, and J. Baptista, “Optimal Cable Design of Wind Farms: The Infrastructure and Losses Cost Minimization Case,” *IEEE Trans. Power Syst.*, vol. 31, no. 6, pp. 4319–4329, 2016, doi: 10.1109/TPWRS.2016.2521700.
[52] W. Musial and B. Ram, “Large-Scale Offshore Wind Power in the United States,” 2010.
[53] C. Mone, T. Stehly, B. Maples, and E. Settle, “2014 Cost of Wind Energy Review,” 2015.
[54] IRENA, “Renewable Energy Technologies: Cost Analysis Series - Volume 1: Power Sector, Issue 5/5 Wind Power,” 2012.
[55] P. Vithayasrichareon, G. Mills, and I. F. MacGill, “Impact of Electric Vehicles and Solar PV on Future Generation Portfolio Investment,” *IEEE Trans. Sustain. Energy*, vol. 6, no. 3, pp. 899–908, Jul. 2015, doi: 10.1109/TSTE.2015.2418338.
[56] W. Li, K. He, and Y. Wang, “Cost comparison of AC and DC collector grid for integration of large-scale PV power plants,” *J. Eng.*, vol. 2017, no. 13, pp. 795–800, Jan. 2017, doi: 10.1049/joe.2017.0440.
[57] R. Fu, D. Feldman, and R. Margolis, “U.S. Solar Photovoltaic System Cost Benchmark: Q1 2018,” 2018.
[58] X. Xiang, M. M. C. Merlin, and T. C. Green, “Cost analysis and comparison of HVAC, LFAC and HVDC for offshore wind power connection,” *IET Conf. Publ.*, vol. 2016, no. CP696, pp. 14–19, 2016, doi: 10.1049/cp.2016.0386.
[59] S. Hardy, K. Van Brusselen, S. Hendrix, D. Van Hertem, and H. Ergun, “Techno-Economic Analysis of HVAC, HVDC and OFAC Offshore Wind Power Connections.,” in *2019 IEEE Milan PowerTech*, 2019, pp. 1–6, doi: 10.1109/PTC.2019.8810500.
[60] S. Kim, A. Yokoyama, Y. Takaguchi, T. Takano, K. Mori, and Y. Izui, “Economic Analysis on Multi-Terminal VSC HVDC Systems with Wind Farms based on Hierarchical Optimal Power Flow with Stability Constraint,” in *2019 IEEE Milan PowerTech*, 2019, pp. 1–6, doi: 10.1109/PTC.2019.8810553.
[61] P. Bresesti, W. L. Kling, R. L. Hendriks, and R. Vailati, “HVDC connection of offshore wind farms to the transmission system,” *IEEE Trans. Energy Convers.*, vol. 22, no. 1, pp. 37–43, 2007, doi: 10.1109/TEC.2006.889624.
[62] J. Ruddy, R. Meere, and T. O’Donnell, “A Comparison of VSC-HVDC with Low Frequency AC for Offshore Wind Farm Design and Interconnection,” *Energy Procedia*, vol. 80, pp. 185–192, 2015, doi: 10.1016/j.egypro.2015.11.421.
[63] A. Alassi, S. Bañales, O. Ellabban, G. Adam, and C. MacIver, “HVDC Transmission: Technology Review, Market Trends and Future Outlook,” *Renew. Sustain. Energy Rev.*, vol. 112, no. June, pp. 530–554, Sep. 2019, doi: 10.1016/j.rser.2019.04.062.
[64] J. Goncalves, D. J. Rogers, and J. Liang, “Extension of power transmission capacity in MMC-based HVDC systems through dynamic temperature-dependent current limits,” in *2015 17th European Conference on Power Electronics and Applications (EPE’15 ECCE-Europe)*, 2015, pp. 1–10, doi: 10.1109/EPE.2015.7309159.
[65] B. Zakeri and S. Syri, “Electrical energy storage systems: A comparative life cycle cost analysis,” *Renew. Sustain. Energy Rev.*, vol. 42, pp. 569–596, Feb. 2015, doi: 10.1016/j.rser.2014.10.011.
[66] L. Barelli, G. Bidini, and F. Bonucci, “A micro-grid operation analysis for cost-effective battery energy storage and RES plants integration,” *Energy*, vol. 113, pp. 831–844, 2016, doi: 10.1016/j.energy.2016.07.117.
[67] M. Farhadi and O. Mohammed, “Energy Storage Technologies for High-Power Applications,” *IEEE Trans. Ind. Appl.*, vol. 52, no. 3, pp. 1953–1962, 2016, doi: 10.1109/TIA.2015.2511096.
[68] C. S. Lai and M. D. McCulloch, “Levelized cost of electricity for solar photovoltaic and electrical energy storage,” *Appl. Energy*, vol. 190, pp. 191–203, Mar. 2017, doi: 10.1016/j.apenergy.2016.12.153.
[69] H. G. Lee, G. G. Kim, B. G. Bhang, D. K. Kim, N. Park, and H. K. Ahn, “Design Algorithm for Optimum Capacity of ESS Connected with PVs under the RPS Program,” *IEEE Access*, vol. 6, pp. 45899–45906, 2018, doi: 10.1109/ACCESS.2018.2865744.
[70] P. K. S. Roy, H. B. Karayaka, Y. Yan, and Y. Alqudah, “Investigations into best cost battery-supercapacitor hybrid energy storage system for a utility scale PV array,” *J. Energy Storage*, vol. 22, no. December 2018, pp. 50–59, Apr. 2019, doi: 10.1016/j.est.2018.12.024.
[71] E. Chatzinikolaou and D. J. Rogers, “A Comparison of Grid-Connected Battery Energy Storage System

Designs," *IEEE Trans. Power Electron.*, vol. 32, no. 9, pp. 6913–6923, 2017, doi: 10.1109/TPEL.2016.2629020.